Isotope-Geochemical Composition, Mineralogy, and Genesis of Mn-Bearing Rocks of the Gondite Association of the Ikat Terrane (Eastern Baikal Region)

S.I. Shkol'nik[a, ✉], I.G. Barash[a], M.D. Buyantuev[b]

[a] *Institute of Earth Crust, Siberian Branch of the Russian Academy of Sciences, ul. Lermontova 128, Irkutsk, 664033, Russia*

[b] *Geological Institute, Siberian Branch of the Russian Academy of Sciences, ul. Sakhyanovoi 6a, Ulan-Ude, 670047, Russia*

Abstract— We present data on the mineral and geochemical compositions of metasedimentary Mn-bearing rocks of the Itantsa Formation of the Ikat terrane. According to the mineral composition, the studied quartz–spessartine rocks of the formation are referred to as gondites. The main Mn-concentrating minerals are garnet, pyrophanite, and Mn-ilmenite, and the secondary ones are rhodonite and Mn-amphibole. Two Mn-bearing objects of the Itantsa Formation (Usutai deposit and Almarnatol occurrence) show differences in chemical and mineral compositions, related to different sources of their material, different distances from the mouth of a hydrothermal vent, and different degrees of postsedimentary alteration. The Mn-bearing deposits of the formation accumulated in a sedimentary basin in the immediate vicinity of continental provenance areas in the Late Neoproterozoic (Ediacaran), under synchronous volcanic activity.

Keywords: gondites, Ikat terrane, Itantsa Formation, geochemistry, mineralogy, formation conditions

INTRODUCTION

The Vendian–Cambrian Earth formation stage coincides with planetary climatic changes, biosphere evolution, wide-scale glaciations with the following postglacial transgressions; the global epoch of manganese accumulation is also associated with this time. That time-period, formation of large manganese deposits of the Far East, the Yenisei Ridge, Altai–Sayan folded area and the Baikal manganese provinces took place in the paleo-Asian part of the planet (Golovko et al., 1982; Gurvich et al., 1982; Rakhmanov et al., 1982; Kuleshov, 2011; etc.). Wide propagation of manganese-bearing rocks and their assignment to different thicknesses by origin and geological structure are the most typical for the Baikal-adjacent part of the Central Asian mobile belt (Betekhtin, 1946; Belichenko, 1969; Osokin et al., 1989; Koneva et al., 1998; etc.). All ore occurrences tend to distribute within thick volcanosedimentary sequences of the terranes (Khamardaban, Olkhon, and Ikat), whose degree of metamorphic change varies from greenschist to granulitic.

The Slyudyanka manganese ore occurrence known within the Khamar-Daban composite terrane is located in the lower part of the terrigenous-carbonate Khangarul Group (Vasil'ev et al., 1981). The most widespread type of manganese containing rocks are diopside gneisses and crystalline schists as well as gondites (quartz-garnet rocks), marbles and calcifires with minerals of the bustamite-wollastonite series. Concentrations vary from several to 20–25 wt.% of MnO. The state of knowledge of the occurrence is rather good, especially concerning those rock associations that are close to gondites (Koneva et al., 1998).

A number of Mn-bearing sequence occurrences have been found in one of the tectonic units (the Anginsk sequence) of the Olkhon metamorphic terrane, where the Tsagan-Zaba ore occurrences is the largest (Betekhtin, 1946). Ores are distributed in the marble sequence and represented by carbonate, carbonaceous–siliciclastic and silicate varieties with MnO content up to 40% (Shkol'nik and Letnikova, 2015). The rocks of the gondite association were found here (Koneva et al., 1998).

The Ikat terrane is characterized by the presence of numerous ore occurrences with inherent manganese and ferromanganese mineralization. The Taloi and Podikat deposits of the Ikat Ridge, the Usutai deposit and the Almarnatol occurrence of the Morskoi Ridge are considered to be the main among them. The Podikat deposit is assigned to the Ikat Formation, which is represented by a sequence of siliceous and carbonate varieties sometimes with silt admixtures. The content value of manganese oxides in the rocks sometimes reaches 30% and more (Shkol'nik and Letnikova, 2015). Manganese rocks of the Morskoi Ridge tend to develop within the borders of the effusive-carbonate-shale lithological complex of the Itantsa Formation (Gusev et al., 1970; Osokin et al., 1989). The detailed mineralogical and geochemical analyses of ore-bearing deposits of the Itantsa Formation have revealed the existence of varieties, which could be referred to gondite associations, among the significant diversity of Mn-containing rocks.

✉Corresponding author.
E-mail adress: sink@crust.irk.ru (S.I. Shkol'nik)

The term gondite was for the first time applied to metamorphic Mn-bearing sedimentary quartz-spessartine rocks (Fermor, 1909). Hereafter, rocks with the same composition were found in most Indian and world Mn-bearing units; their compositional characteristics and the term limits have been the subject of numerous discussions (Varentsov, 1962; Roy, 1969; Kulish, 1973; Reznitsky et al., 1976; Golovko and Ikonnikova, 1977; Dasgupta et al., 1990; Koneva et al., 1991; Melcher, 1995; etc.). Gondites are considered as metamorphized aluminosilicate sedimentary rocks primarily enriched with manganese, which do not contain carbonate material in noticeable quantities. Besides two main minerals—quartz and spessartite, the mineral composition of gondites can include pyroxmangite, rhodonite, manganese clino- and orthopyroxene, Mn-amphiboles and a number of manganese micas analogs, epidote and others (Roy, 1965; Melcher, 1995; Mohaparta and Nayak, 2005; etc.). Mn-ilmenite and pyrophanite, and braunite, hollandite, jacobsite, hausmannite are of frequent occurrence among the oxides.

Besides the gondites, spessartine quartz, carbonate-free shale with predominant concentration of alumosilicates (partially manganous) are often referred to the gondite association. In cross-sections, gondites could alternate with calcareous-silicate rocks and (that is particularly important) with interbedding bodies of endogenous ores, which are mostly of production type (Shkol'nik et al., 2017).

The rocks of the gondite composition are observed in various units depending on the extent of metamorphic changes, for instance from greenschist to granulite. Host units compositions similar to chemical characteristics of gondites can vary within a broad range. Mineral and chemical composition of the gondite association in the metamorphic sequences next to the Baikal Region (Pribaikalia) was analyzed within the borders of the Olkhon and Khamar-Daban terranes (Koneva et al., 1998). Based on the analysis data, the conclusion was drawn that all these associations belong to a single regional level of manganese accumulation. The study presents the updated information on mineral, geochemical and isotope composition of quartz-spessartine rocks of the Ikat terrane; it also provides the comparison of their geochemical parameters with the gondites of the Khamar-Daban and the Olkhon terranes.

THE IKAT TERRANE STRUCTURE AND THE GEOLOGICAL POSITION OF Mn-BEARING ROCKS

The Ikat terrane lies in the northeast part of the Baikal mountain area and shares rather conventional borders with Barguzin, Khamar-Daban, Eravna, and Olkhon terranes of the Central Asian fold belts (Fig. 1). Stratified units are split into several groupes or formations, which are comprised of mostly carbonate rocks. The Ikat, Kurba, and Selenga areas are clearly distinguished within its structure. They were earlier identified as structural-formational zones, which are re-
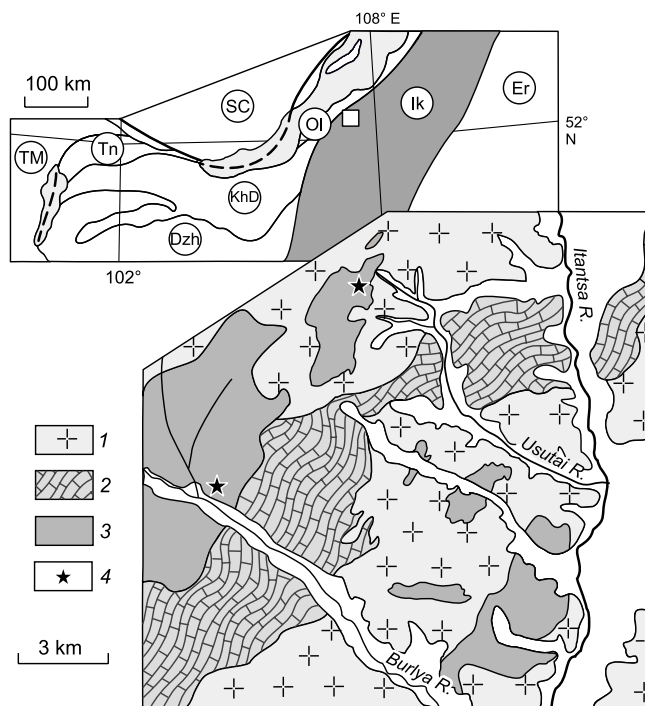

Fig. 1. The terranes outline of the Baikal–Khubsugul Region; a schematized geological map of the area along the Burlya and Usutai Rivers; (approximated from (Gusev, 1970)).

stored by the fragments of constituting deposits, in the very wide granitoid field of the Angara–Vitim batholith (Belichenko et al., 2006). The Selenga area which is distinguishable by a more complex structure and spatially constrained by the Morskoi Ridge is represented by volcanosedimentary deposits of the Itantsa and Burlya Formations. The Itantsa Formation is characterized by the significantly mixed character of lithological composition and its variability in the lateral direction (Osokin et al., 1989). The following complexes can be identified within its composition: shaly–carbonate, quartzite–sand–shale, carbonate–siliceous–shale and carbonate–effusive–shale lithofacial complexes. The horizons of monomineral quartz sandstones, apatite-containing rocks, and highly-graphitic shales are the most typical for the formation. Making up the bulk of the formation composition, the rocks of the carbonate-effusive-shale complex are represented by mafic metaeffusives, which interlay with argillaceous-siliceous and carbonate rocks (Osokin et al., 1989). Less developed are biotite gneisses and quartz-type sandstones. Having a regular overlap with the Itantsa Formation, the Burlya Formation is represented by carbonate rocks with horizons of carbonaceous-argillaceous and P-bearing rocks. Cambrian fauna was found in the carbonate rocks (Belichenko, 1969). The formation metamorphism tends to increase towards the boundary with the Olkhon terrane.

The exploration was conducted within the carbonate–effusive–shale complex to which ore-grade manganese occurrences were assigned. The complex rocks form an extended narrow stripe with the exposure of manganese occurrences

confined to its edges (Usutai and Almarnatol) that is cut off by outcropping of granitoids. The Mn-bearing sequence is embedded among silicious-, sercite-chlorite and actinolite shales within the Almarnatol occurrence. Quartz-biotite hornfels and amphibolites are the host rocks for ferromanganese ores of the Usutai deposit. The analysis of mineral-geochemical composition of manganese rocks has revealed that there are rock varieties which could be referred to as gondites among their remarkable diversity, including the rocks, whose lithological and mineralogical aspects have been studied in details (Gusev et al., 1970; Osokin et al., 1989).

MANGANESE ROCKS OF THE IKAT TERRANE

Almarnatol occurrence. The occurrence appears to be a sequence of manganese rocks with the width of the first tens of meters, which is embedded among silicious-, sercite-chlorite and actinolite shales. Gondites are represented by thin-striped fine-grained rocks, which are mainly composed of quartz and garnets that could be enriched with biotite and ilmenite in separate sequences (Fig. 2*a*). Gondites can some-

times form thin yellowish beds (up to 3 cm wide) in quartz micaceous shale; they mainly contain garnets and small concentrations of quartz (Fig. 2*b*). Garnet is one of the main gondite constituents; it tends to form automorphic grains or clusters in size of 20 to 50–70 µm (Fig. 3*a*). Fine garnet grains often create discontinued practically mono-mineral chains alternating with stripes of quartz (Fig. 3*b*). Regarding composition, it is referred to the almandine-spessartine (Table 1) series with the content of the spessartite-minal reaching up to 60%, and the almandine-minal up to 33%, and the andradite-minal is also present in the garnet composition in significant quantities (up to 20%) (Fig. 4). Mn-ilmenite always occurs as an auxiliary mineral, which has not been detected in the manganese rocks of the Almarnatol occurrence before. Mn-ilmenite combined with garnet and quartz can sometimes form thin enriched stripes (Fig. 2*a*) which sharply differ in color. However, they tend to occur in the form of sparse fine grains among garnet stripes (Figs. 2*b*, 3*b*) or in the form of thin (thousandths of mm) inclusions (Fig. 3*a*) in garnet. Its composition is characterized by high concentration of iron (up to 40%) and variable manganese concentrations (from 8 to 19%) (Table 1). According to (Fig. 5, Table 1), it's likely to be a manganese variety of
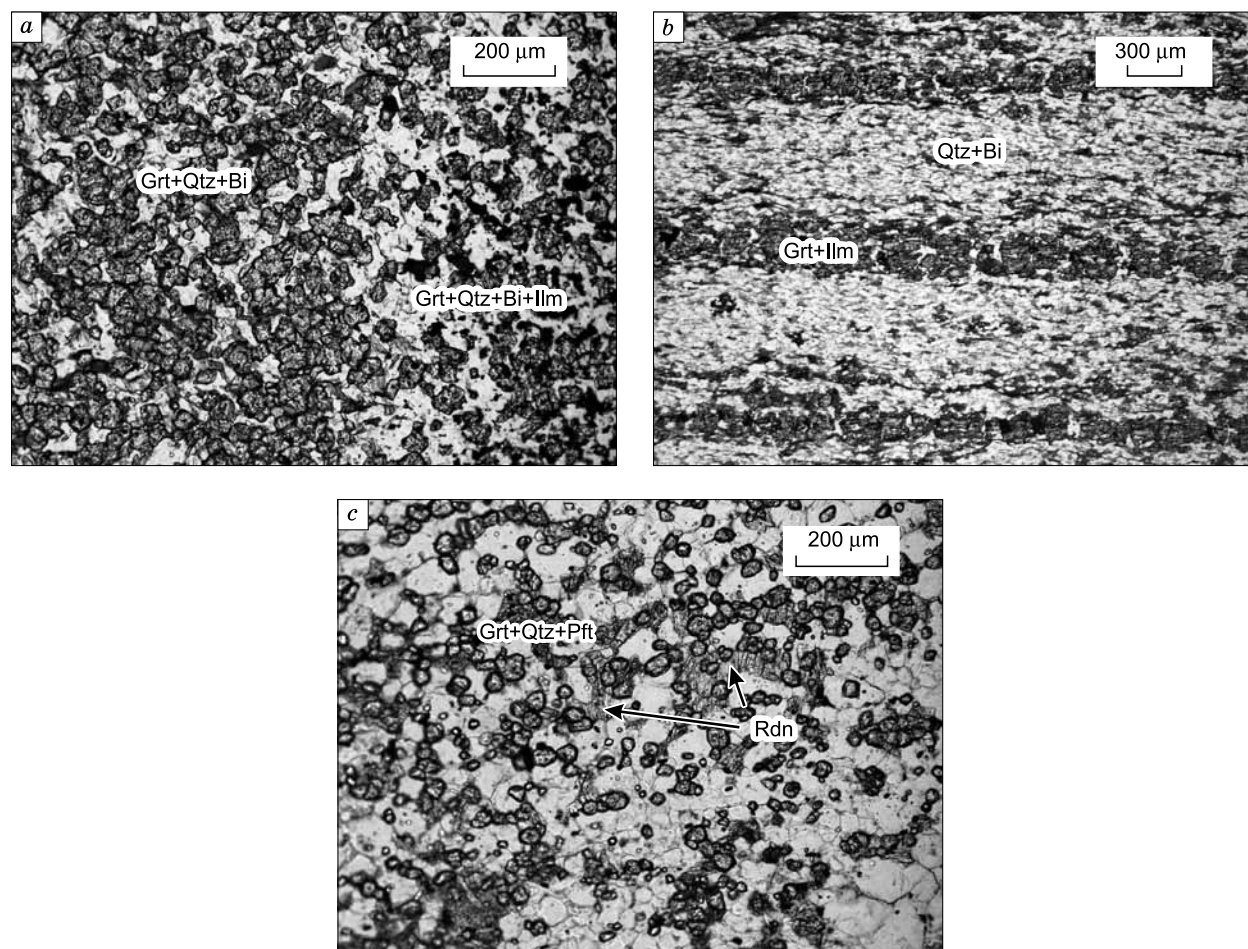
Fig. 2. Gondites of the Itantsa Formation. Massive (*a*) and thin-striped (*b*) gondites of Almarnatol occurrence; *c*, gondite of the Usutai deposit. Minerals: Grt, garnet, Qtz, quartz, Bi, biotite, Ilm, ilmenite, Pft, pyrophanite, Rdn, rhodonite.
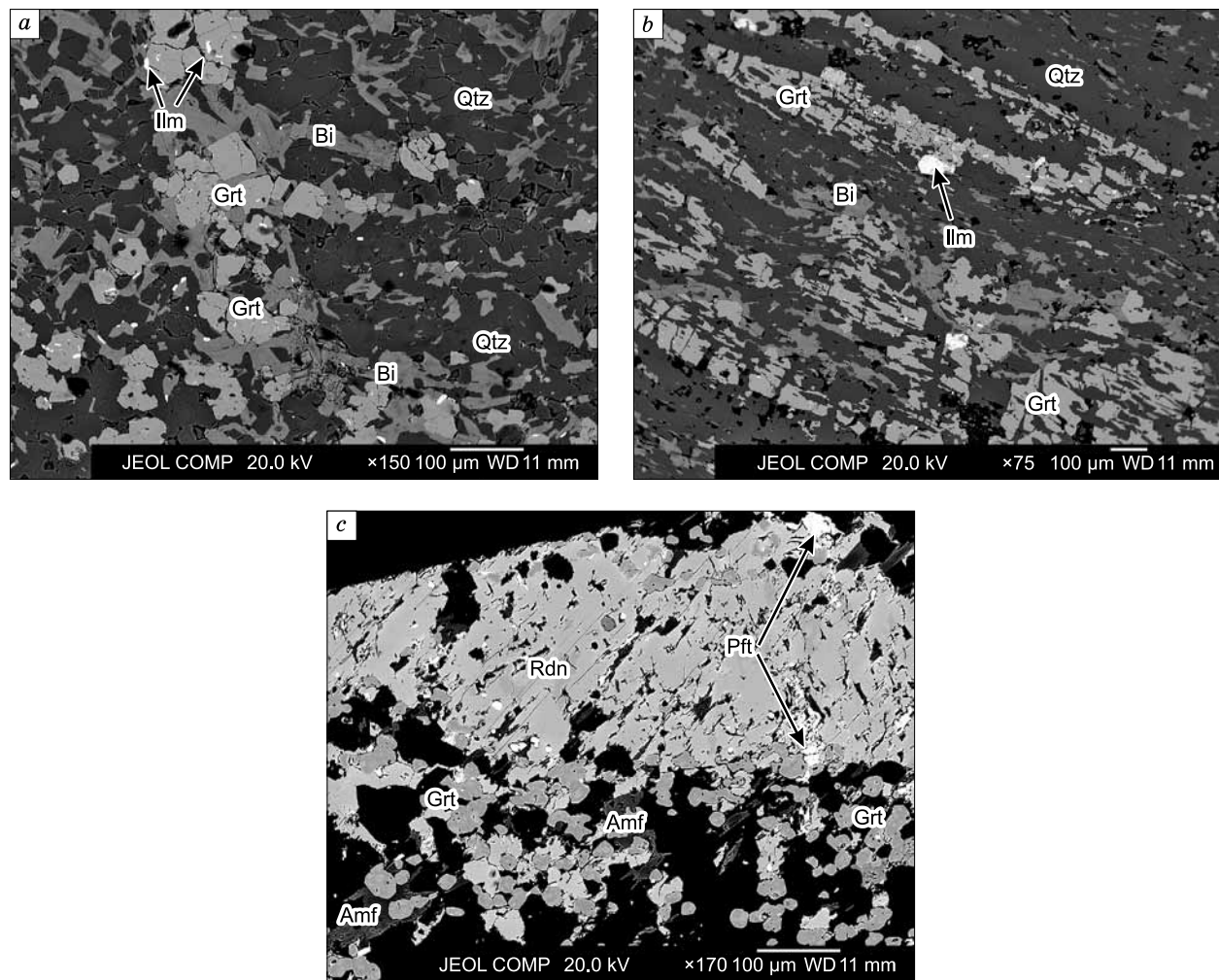
Fig. 3. Mineral associations of gondites from the Almarnatol occurrence (*a*, *b*) and the Usutai deposit (*c*).

ilmenite. Wide development of oxidation zone minerals represented by psilomelane and pyrolusite is typical for Almarnatol ore occurrence (Osokin et al., 1989).

The Usutai manganese deposit. The deposit appears to be a producing sequence consisting of lens- and sheet-like ore bodies mostly made up of biotite-quartz hornfels and ortoamphibolite (Gusev, 1970). Formation of rhodonite hornfels is connected with metamorphism due to intrusions of the Paleozoic granitoids; moreover, primary ore-bearing sediments were of volcanosedimentary nature (Gusev, 1970; Osokin et al., 1989). The rocks of the gondite composition were assigned to the amphibolites of the Itantsin Formation, which was situated at a distance from granite intrusions. Microscopically, they are fine/medium-grained rocks with well-defined garnet grains. In accord with the range of manganese minerals, the gondites from the Usutai deposit differ from that of the Almarnatol occurrence. Except for the main minerals of gondites, i.e., quarts and garnet which account for up to 90% of the rock, the presence of other rock-forming manganese minerals (rhodonite, amphibole, and pyrophanite) is also detected. Consequently, according to the clas-

sification (Melcher, 1995), they are referred to the multimineral type of gondites. Garnet forms well-polished or rounded crystals enclosed in the quartz matrix (Fig. 2*c*) and characterized by high grade of spessartine minal concentration (up to 75%), at nearly equal percentage of andradite and almandine components (up to 20%) and low grossularite content (Fig. 4). Rhodonite forms irregular or tabular different-sized grains (occasionally rather large), which are distributed unevenly in the rock (Fig. 3*c*). Its composition is relatively stable and differentiates only by some fluctuations in the content of iron and manganese (Fig. 6, Table 1). Amphibole forms different-sized grains enclosed in the quartz-garnet matrix, or thin blades in rhodonite. It is close to Mn-cummingtonite in composition (the former name—tyrodite) but differs in fluctuations of MgO and MnO concentrations (Fig. 7). The minerals of the oxidation zone are represented by coronadite, psilomelane, cryptomelane and black oxide of manganese (Osokin et al., 1989).

In contrast with the Almarnatol occurrence, where Mn-ilmenite was detected, the gondites of the Usutai deposit contain pyrophanite, whose composition is characterized by

**Table 1.** Microprobe analyses of garnet from gondites of the Ikat terrane (wt.%), selective sampling

Component	Garnet (Usutai deposit)						Garnet (Almarnatol occurrence)					
SiO_2	36.82	37.14	36.93	36.87	37.15	36.53	35.96	36.69	36.89	36.31	36.40	36.16
TiO_2	0.23	0.21	0.33	0.21	0.29	0.16	0.49	0.19	0.14	0.27	0.11	0.05
Al_2O_3	20.09	19.89	20.22	20.10	20.04	18.55	19.98	19.97	20.30	21.20	21.19	20.52
FeO	4.79	4.81	4.81	5.30	4.53	9.31	15.65	14.15	18.42	12.05	17.24	11.05
MnO	34.28	33.89	34.04	34.01	34.29	30.15	23.47	24.49	19.05	26.93	22.25	29.20
MgO	1.13	0.95	0.92	1.06	1.06	1.38	0.42	0.35	0.54	0.20	0.46	0.22
CaO	2.47	2.82	2.90	2.75	2.37	4.08	3.33	3.96	4.25	3.23	2.55	3.16
Total	99.81	99.75	100.15	100.30	99.75	100.27	99.30	99.80	99.59	100.19	100.20	100.36
Atomic coefficients in the formula (per 12 atoms of oxygen)												
Si	3.008	3.033	3.006	3.002	3.029	3.005	2.973	3.010	3.016	2.961	2.969	2.965
Ti	0.001	0.000	0.001	0.001	0.001	0.000	0.001	0.001	0.000	0.001	0.000	0.000
Al	1.934	1.915	1.939	1.929	1.926	1.798	1.947	1.930	1.955	2.037	2.037	1.983
Fe	0.327	0.329	0.328	0.360	0.310	0.634	1.082	0.970	1.260	0.821	1.176	0.758
Mn	2.372	2.344	2.346	2.346	2.369	2.101	1.643	1.701	1.319	1.860	1.537	2.027
Mg	0.138	0.115	0.111	0.129	0.129	0.169	0.052	0.043	0.066	0.024	0.055	0.027
Ca	0.216	0.246	0.253	0.239	0.207	0.359	0.295	0.348	0.372	0.282	0.223	0.278
Total	7.996	7.982	7.984	8.006	7.971	8.072	7.993	8.003	7.989	7.986	7.987	8.038
Volume components (wt. %)												
Almandine	10.3	10.3	10.3	11.2	9.8	18.2	29.5	27.1	33.6	23.4	31.6	21.7
Pyrope	4.3	3.7	3.5	4.0	4.1	4.8	1.4	1.2	1.8	0.6	1.4	0.8
Spessartine	74.3	74.0	73.6	72.8	75.1	59.8	44.8	47.5	35.3	53.0	41.3	57.9
Grossular	2.0	2.7	3.9	1.8	2.6	0	3.9	5.1	7.7	10.0	7.7	4.6
Schorlomite	0.4	0.3	0.5	0.4	0.5	0.3	0.7	0.3	0.2	0.4	0.2	0.1
Andradite	8.7	9.0	8.2	9.8	7.9	16.9	19.7	18.8	21.4	12.6	17.8	14.9

Note. Here and in the Tables 2 and 3 the analyses were carried out with the use of the Superprobe JXA-820 Jeol electron probe microanalyzer at the Institute of Geochemistry SB RAS (Irkutsk). Analyst L.F. Suvorova.
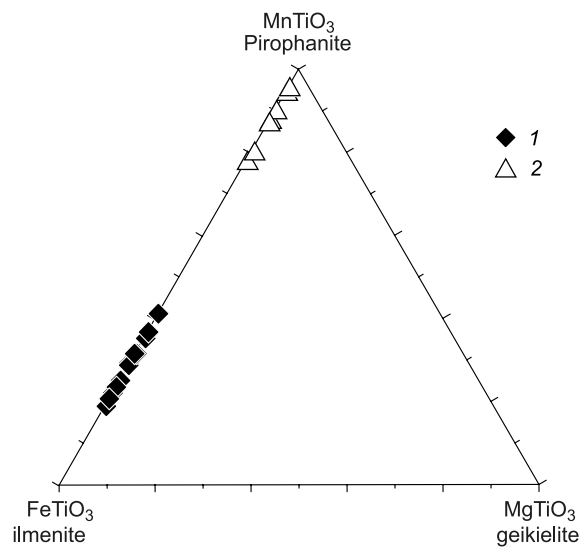
a high content value of manganese (up to 40%) and low concentration of iron (up to 10%) (Table 1). Mn-ilmenite appears to be an intermediate constituent of the solid solutions series as follows: pyrophanite ($MnTiO_3$)–ilmenite($FeTiO_3$). Mn-ilmenite formation ($MnTiO_3$ is below 50 mol.%) occurs in the result of the partial substitution of divalent iron with manganese contained in ilmenite (Deer et al., 1963; Bowles et al., 2011). Mn-ilmenite is a rather common variety of ilmenite not only for manganese formations. It occurs frequently together with pyrophanite (or without it) in rocks of different genetic types, such as ultrabasites (Osipenko and Sidorov, 1999), granites (Czamanske and Mihalik, 1972) and often in adamellites (Snetsinger, 1969). The compositional differences of the main rock-forming mineral phases of the two manganese occurrences (Mn-ilmenite and pyrophanite) are especially related to differences in the protolith composition within the formation borders.

RESEARCH METHODS

The concentrations of petrogenic components were determined by a classic method of "solution chemistry", and concentrations of rare elements were obtained by optical spec-
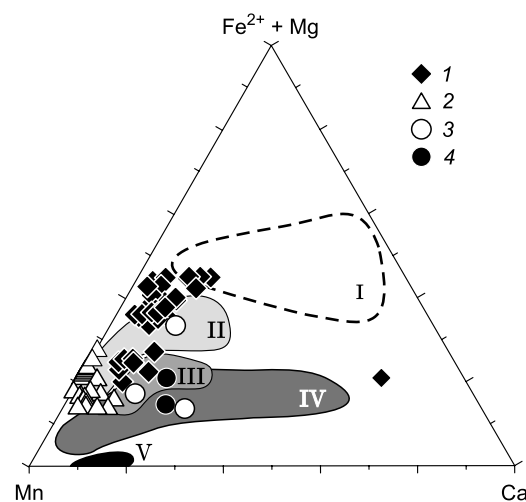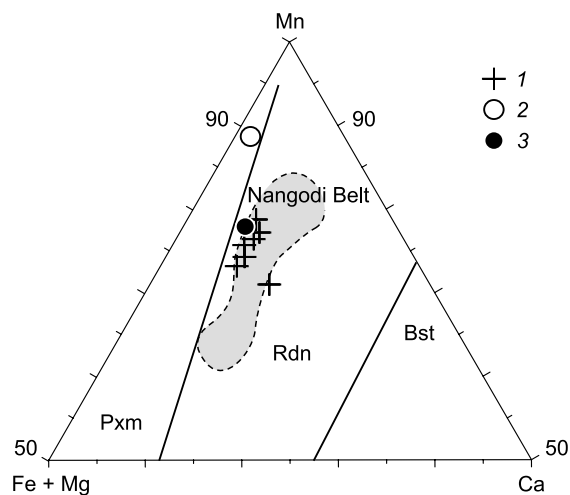

Fig. 4. Composition of garnet from the gondites of the Itantsa Formation. *1*, Almarnatol occurrence; *2*, Usutai deposit. Garnet compositions from gondites of the Olkhon (*3*) and Khamar-Daban (*4*) terranes are given for comparison (Koneva et al., 1998). The fields of mineral manganese associations of gondites from Northern Ghana are represented (Melcher, 1995): I, garnet-containing chlorite shales, II, garnet-quartz-ilmenite (pure) gondites (distal deposits), III, garnet-quartz-amphibole-hyalophane-rhodonite (multimineral gondites), IV, garnet-quartz-amphibole-rhodonite (multimineral gondites), V, garnet-amphibole-rhodonite (proximal deposits).

Fig. 5. Composition of Mn-ilmenite from gondites of the Itantsa Formation. *1*, Almarnatol occurrence; *2*, Usutai deposit.

The microprobe studies were carried out at the Institute of Geochemistry SB RAS (Irkutsk, analyst L.F. Suvorova). Polished thin sections were studied with the use of a JXA-8200, Jeol electron probe microanalyzer fitted with the high-resolution scanning electron microscope, the energy dispersion spectrometer with SiLi detector with resolution of 133 EV and five spectrometers with wave dispersion. An internal grain structure was studied with the scanning electron microscope with SEM images obtained by secondary electrons (SE) and back-scattered electrons (BSE) technique at different degrees of magnification; the elements distribution was detected with characteristic X-rays. The quantitative analysis was carried out with the use of a spectrometer with wave dispersion under the following analytic conditions: accelerating voltage of 20 kV, electron beam current of 20 nA, probe diameter of 1 μm, pulse count time—10 s at the peak on the line, the background was measured from both sides of the line for 5 s. The company's licensed software was applied to compute chemical content of minerals; natural minerals and artificial compounds (attested as laboratory samples) were used for calibration.

Isotope research was done at the Geodynamics and Geochronology CUC of IEC SB RAS (Irkutsk). The samples were prepared in accord with the following pattern. The weight of 100 mg of the ground sample was decomposed in the acid mixture of HNO_3–HF–$HClO_4$ in a microwave oven. Definition/separation of REE was carried out on TRU Spec resin (EIChroM Industries, II. USA). Next, Sm and Nd partition was conducted on the column filled with Ln Spec resin in accord with the modified methodology (Pin and Zalduegui, 1997). Measurements of isotope Nd ratios were done with the Finnigan MAT-262 device. In the result of mass-spectrometry measurements the isotope relations were normalized by: $^{146}Nd/^{144}Nd = 0.7219$. Fractionation correc-
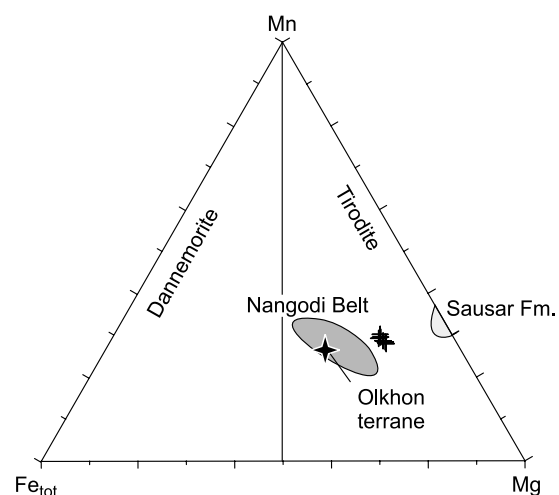
trum and X-ray fluorescence analyses. All the analyses were conducted at the "Geodynamics and Geochronology" CUC of the IEC SB RAS (Research Associates: G.V. Bondareva, E.V. Khudonogova, S.I. Shtelmakh, V.V. Shcherban', A.V. Naumova, L.V. Vorotynova). Concentrations of REE elements, U, Th, and Cs were determined by ICP-MS method; the methodology is described in (Panteeva et al., 2003). The measurements were carried out at "Ultramicroanalysis" OU CUC with an Agilent 7500 quadrupole mass-spectrometer (Agilent Technologies Inc., USA) with the use of international and Russian standards (BHVO-2, RCM-1, JG-2 and others). The admissible error limit for concentrations detection does not exceed 10%.

Fig. 6. Composition of rhodonite on the diagram Ca–Mn–Fe + Mg (Winter et al., 1981) from gondites. *1*, Usutai deposit; *2*, Olkhon terrane; *3*, Khamar-Daban terrane in accord with (Koneva et al., 1998). The field of rhodonite composition from Nangodi Belt (Melcher, 1995) is represented. Minerals: Rdn, rhodonite, Pxm, pyroxmangite, Bst, bustamite.

Fig. 7. Composition of amphibole on the diagram Mg–Mn–Fe_{tot} from gondites: Usutai deposit (crosses), Olkhon terrane in accord with (Koneva et al., 1998) and from the Nangodi Belt and the Sausar Formation in accord with (Melcher, 1995). Minerals: Rdn, rhodonite, Pxm, pyroxmangite, Bst, bustamite.

tion was carried out by Rayleigh law. To control the device operation quality, neodymium standard JNd-1 was measured; within the measurement period its value was equal to: $^{143}Nd/^{144}Nd = 0.512070 \pm 10$.

Preliminary preparation of the samples and partition of accessory zircon were fulfilled at CUC of IEC SB in compliance with the standard methodology. U–Pb geochronological dating of zircons from gneiss of the Itantsa Formation was carried out at the Geological Institute SB RAS (Ulan-Ude); the detailed methodology description is in (Khubanov et al., 2016).

ISOTOPE GEOCHEMICAL CHARACTERISTICS OF MANGANESE-BEARING ROCKS

Manganese-bearing rocks (gondites) of the Usutai and Burlya river basins are characterized by different content of SiO_2 (57–68 and 60–92 wt.%), CaO (1.5–7.0 and 0.5–2.5 wt.%), MgO (2.6–3.0 and 0.1–1.4 wt.%), MnO (3–10 and 1.5–6.0 wt.%) and K_2O (0.4–0.9 and 0.2–2.8 wt.%), and also by significant variations in concentrations of Al_2O_3, TiO_2, Na_2O, and iron (Table 2). Estimation of the contribution to deposit composition of lithogenetic unit/component is based as a rule on definition of aluminum and titanium content. The existing direct correlation between the concen-

trations of these components in the analyzed manganese deposits (Fig. 8a) indicates that the formation took place in the result of significant contribution to the terrigenous material. In this case, the inverse correlation between silicon and aluminum concentrations (Fig. 8b) supposes their accumulation to be related to different sources of substances contribution to the sedimentation basin. Significant silicon excess in relation to aluminum (Si:Al more than 5:1; that is higher compared with this relation for pelagic clays (Brusnitsyn, 2015)) implies the existence of various terrigenous provenance areas, or silicon contribution through hydrothermal solutions. The use of diagrams for partition of sedimentary and hydrothermal silicites (Fig. 9) has shown that the most part of the studied manganese deposits is localized in the proximity to the field of sedimentary rocks with a significant concentration of hydrothermal material impurities. The contribution of the hydrothermal substance is usually determined by concentrations of such elements as iron and manganese. To solve the problem, Strakhov module (Fe + Mn/Ti) (Strakhov, 1976) and Boström module Al/(Al + Fe + Mn) (Boström, 1974) are conventionally applied according to (Butuzova, 1998; Gurvich et al., 1998). Based on the values analysis of the given modules, hydrothermal sedimentary deposits could be split into ore-bearing ((Fe + Mn/Ti) > 100 and Al/(Al + Fe + Mn) < 0.1) ((Fe + Mn/Ti) > 100 and Al/(Al + Fe + Mn) < 0.1) and metal-bearing (Fe + Mn/Ti) 25–

Table 2. Microprobe analyses of Mn-ilmenite and pyrophanite from gondites of the Ikat terrane (wt.%), selective sampling

Component	Pyrophanite (Usutai deposit)						Mn-ilmenite (Almarnatol occurrence)					
SiO_2	0.09	0.23	0.92	0.11	0.14	0.25	0.20	0.67	0.65	0.01	1.60	0.19
TiO_2	52.41	49.93	51.44	51.90	50.41	50.48	51.16	51.33	53.43	51.55	51.57	52.37
Al_2O_3	0.03	0.08	0.10	0.00	0.03	0.00	0.00	0.24	0.04	0.04	0.06	0.03
FeO	2.37	6.24	2.81	2.31	10.77	9.64	28.48	37.84	30.42	37.58	34.72	32.98
MnO	43.59	41.83	42.39	43.51	36.53	38.02	18.99	8.39	13.32	10.07	9.10	12.67
MgO	0.01	0.00	0.00	0.00	0.03	0.20	0.00	0.04	0.00	0.00	0.00	0.00
CaO	0.01	0.04	0.13	0.04	0.11	0.26	0.14	0.27	0.14	0.03	0.00	0.11
V_2O_3	0.00	0.00	0.23	0.18	0.22	0.21	0.21	0.22	0.21	0.24	0.21	0.25
Total	98.51	98.35	98.02	98.05	98.24	99.06	99.18	99.00	98.21	99.52	97.26	98.60
Atomic coefficients in the formula (per 3 atoms of oxygen)												
Si	0.002	0.006	0.023	0.003	0.003	0.006	0.005	0.017	0.016	0.000	0.040	0.005
Ti	1.002	0.967	0.983	0.998	0.976	0.969	0.981	0.978	1.014	0.986	0.987	1.001
Al	0.001	0.002	0.003	0.000	0.001	0.000	0.000	0.007	0.001	0.001	0.002	0.000
Fe	0.050	0.134	0.059	0.049	0.232	0.206	0.607	0.802	0.642	0.799	0.739	0.701
Mn	0.939	0.913	0.912	0.942	0.796	0.822	0.410	0.357	0.285	0.217	0.196	0.273
Mg	0.000	0.000	0.000	0.000	0.001	0.008	0.000	0.001	0.000	0.000	0.000	0.000
Ca	0.000	0.001	0.003	0.001	0.003	0.007	0.004	0.007	0.004	0.001	0.000	0.002
V	0.000	0.000	0.005	0.004	0.004	0.004	0.004	0.004	0.004	0.005	0.004	0.005
Total	1.994	2.023	1.988	1.997	2.016	2.022	2.011	1.999	1.966	2.011	1.970	1.990
Volume components (wt.%)												
$MnTiO_3$	94.9	87.2	93.9	95.1	77.4	79.3	40.3	30.8	30.7	21.4	21.0	28.0
$FeTiO_3$	5.1	12.8	6.1	4.9	22.6	19.9	59.7	69.1	69.3	78.6	79.0	72.0
$MgTiO_3$	0	0	0	0	0	0.8	0	0.1	0	0	0	0
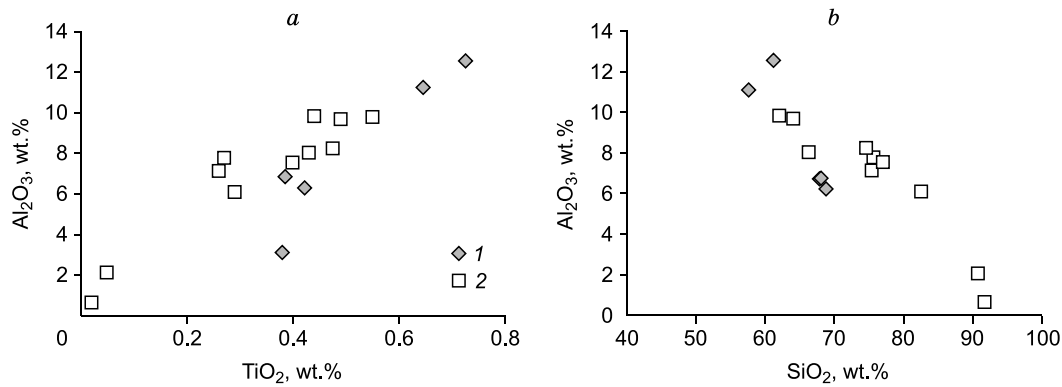
Fig. 8. Diagrams: TiO_2–Al_2O_3 (*a*) and SiO_2–Al_2O_3 (*b*) for manganese rocks of the Itantsa Formation. *1*, Usutai deposit; *2*, Almarnatol occurrence.

100 and Al/(Al + Fe + Mn) 0.1–0.5. Regarding these criteria, all Mn-bearing deposits (with the exception of two samples from the Usutai deposit and Almarnatol occurrence) can be referred to metal-bearing deposits. Geochemical composition is characterized by broad variations in concentrations of the most microelements. In relation to the Almarnatol gondites, lower concentrations of Cs, Rb, Zr, Hf, Th, U, Pb and higher concentrations of Sr, Cr, Co (Fig. 10*a*, Table 1) are the most typical for the Usutai deposit. The common feature for all the Mn-bearing formations of the Itantsa Formation is recognized to be higher or close to PAAS content values of Co, Ni, Cu (Fig. 10*a*).
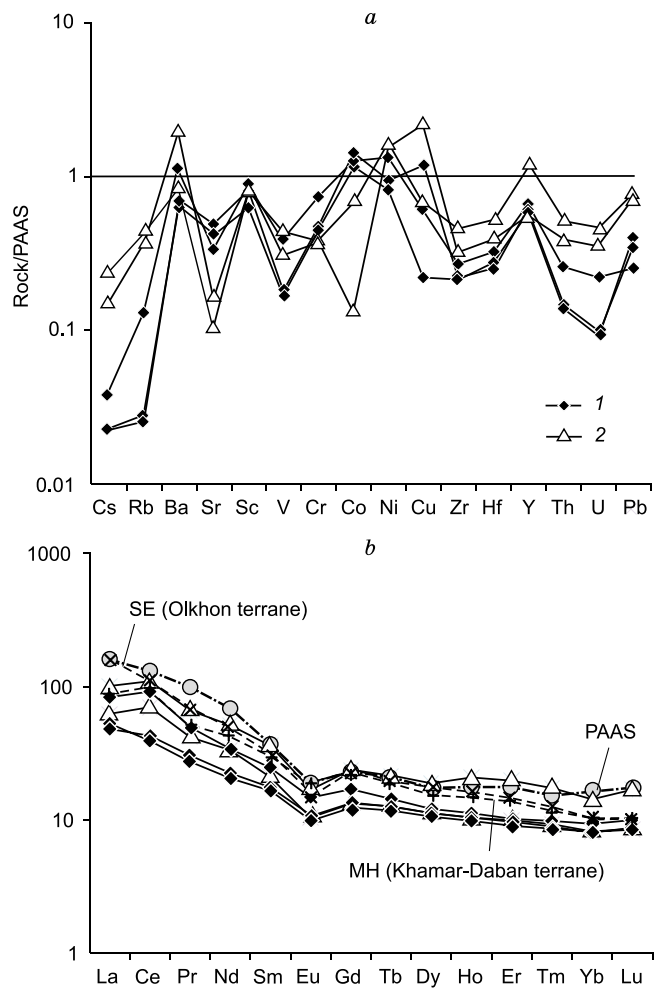
The distribution spectra of rare earth elements (REE) are close to PAAS composition and differ only by REE total amount, and the presence of positive Ce anomaly (Fig. 10*b*). Well-defined Eu anomaly (Eu/Eu* = 0.57–0.72) is mostly common for all the Mn-bearing rocks; moreover, the relation $(La/Yb)_n$ (6.0–8.9) is close to this one in PAAS (9.7).

The obtained Sm–Nd isotopic values are close enough for different ore occurrences. For the Almarnatol occurrence, the estimate of ε_{Nd} (500 Ma) lies in the range of –8.2 to –9.2 (Letnikova et al., 2016) and it varies for the Usutai deposit from –9.0 to –10.3 (Table 3). These estimates are the indicatives of the great effect that both ancient continental

provenance areas and the sedimentation basin location at a relative distance from hydrothermal activity sources had on the formation of the above-mentioned deposits. The ob-

Fig. 10. Distribution spectra of rare elements normalized for PAAS (Taylor and McLennan, 1985) and rare earth elements (REE) normalized for chondrite (Sun and McDonough, 1989) from manganese rocks of the Itantsa Formation. *1*, Usutai deposit; *2*, Almarnatol occurrence. Fig. 10 represents distribution spectra for REE in gondites from the Olkhon (SE) and Khamar-Daban (MH) terranes.

Fig. 9. Diagram (Fe + Mn)/Ti–$(Al_2O_3/SiO_2) \cdot 1000$ (Zaikova, 1991) for manganese rocks of the Itantsa Formation. *1*, Usutai deposit; *2*, Almarnatol occurrence. See Fig. 8 for designations.

Table 3. Microprobe analyses of amphibole and rhodonite from gondites of the Ikat terrane (wt.%), selective sampling

Component	Amphibole (Usutai deposit)						Rhodonite (Usutai deposit)				
SiO_2	54.88	55.14	54.76	54.47	55.11	55.45	49.12	47.84	47.14	49.53	50.56
TiO_2	0.01	0.00	0.04	0.12	0.06	0.06	0.07	0.02	0.05	0.22	0.09
Al_2O_3	0.11	0.12	1.82	0.19	0.19	0.12					
FeO	8.38	8.36	8.06	8.41	8.39	8.74	5.49	4.89	5.14	5.31	4.43
MnO	16.41	15.95	16.36	15.98	16.18	16.33	38.17	40.08	39.11	37.85	41.20
MgO	17.54	17.88	16.98	18.65	18.54	17.55	3.47	2.63	3.58	4.42	2.89
CaO	1.04	0.65	1.56	0.96	0.88	0.74	4.22	4.31	3.79	4.12	3.77
Na_2O	0.09	0.04	0.07	0.07	0.09	0.07					
H_2O	2.06	2.06	2.09	2.07	2.08	2.07					
Total	100.52	100.20	101.74	100.92	101.52	101.13	100.54	99.77	98.81	101.45	102.94
Atomic coefficients in the formula (per 23 atoms of oxygen)							Atomic coefficients in the formula (per 6 atoms of oxygen)				
Si	7.976	8.000	7.843	7.879	7.918	8.002	2.033	2.017	2.004	2.027	2.048
Ti	0.001	0.000	0.004	0.013	0.006	0.006	0.004	0.000	0.003	0.013	0.005
Al	0.018	0.021	0.307	0.032	0.033	0.022					
Fe	1.019	1.015	0.965	1.016	1.008	1.055	0.190	0.173	0.183	0.181	0.150
Mn	2.020	1.962	1.985	1.957	1.969	1.995	1.337	1.432	1.408	1.309	1.413
Mg	3.799	3.869	3.628	4.021	3.969	3.774	0.214	0.165	0.226	0.269	0.175
Ca	0.161	0.101	0.240	0.148	0.135	0.113	0.187	0.194	0.172	0.180	0.163
Na	0.027	0.011	0.018	0.019	0.026	0.020					
Total	15.027	14.988	15.005	15.097	15.073	14.990	3.966	3.982	3.996	3.977	3.953
OH	2.000	2.000	2.000	2.000	2.000	2.000					

tained estimates of model isotopic ages show that both ancient and fresh rocks (probably, volcanics generated subsynchronously to sediment formation) must have been the migration sources. These conclusions are in compliance with the data on U–Pb dating of zircons obtained by LA-ICP-MS method (Shkolnik et al., 2017), which detailed description is given below.

Hence taken for dating from the interstream area of the Usutai and Burlya Rivers, the sample of biotite gneiss is a light gray rock with a well-marked banded structure, which is mainly composed of quartz and feldspar with insignificant fraction of biotite and, in rare cases, of hornblende concentration. 87 zircon grains of gneiss from the Itantsa Formation have been analyzed; 43 zircon grains (51%) revealed concordant age estimates (degree of discordance is ±10%) (Table 4), which were used for constructing the histograms and diagrams of age distribution probability density. The most part of the selected zircons (60–100 μm) is represented by short- and long-prismatic semitransparent crystals (Fig. 11) frequently with oscillating zonation. Large zircons (100–200 μm) account for 10% of the total quantity of the analyzed minerals. They are represented by grains with different degrees of abrasion and sometimes with a well-distinguished metamorphic rim. The concordant ages of the analyzed zircons lie in the intervals of 694–665 (4 grains) and 812–717 (23 grains) Ma with peak values of 0.66 and 0.76 Ga (Fig. 12). In addition, ages of 491 ± 5 Ma and 1938 ± 26 Ma were determined in individual grains. Ancient

zircons form a wide continuous cluster without strongly marked peak values within the range of 2671–2312 Ma (14 grains).

RESULTS AND DISCUSSION

The analysis of the given chemical and mineral compositions of the manganese rocks from the effusive–carbonate–shale lithological complex of the Itantsa Formation of the Ikat terrane has proved the fact that in accord with all the parameters the studied Mn-bearing association of the Usutai deposit and the Almarnatol occurrence correspond to gondites. The differences of mineral and chemical compositions of the Mn-bearing association of the Itantsa Formation are certain to be connected with variations of the initial composition, i.e., the substance source or provenance.

According to (Dubinin, et al., 2008), the main sources of iron-manganese sedimentary depositions are known to be: volcanoterrigenous, hydrogenous and hydrothermal. The gondites of the Usutai deposit differ in chemical composition by low concentrations of silicon, higher content values of MgO, MnO, CaO and lower content values of K_2O. The volcanoterrigenous component of the Mn-bearing deposits takes an important part in accumulation of a series of elements and, in general, it is distinguished by high concentrations of aluminum, titanium, silicon, magnesium, sodium and eventually iron, and other components, but it only slightly influences manganese content (Dubinin, 2008). The

Table 4. Representative analyses of chemical (wt.%) and rare element (ppm) content in Mn-bearing rocks from the Itantsa Formation of the Ikat terrane

Component	I					II								
	BR-23	BR-25	BRL-3	BRL-4	BRL-7	UST-1	UST-14	US-1	US-7	US-9	SE 1165A	MH-130	1	2
SiO_2	77.02	74.58	62.07	66.29	82.55	57.11	61.12	68.44	68.26	68.57	51.17	62.19	69	50
TiO_2	0.40	0.48	0.55	0.43	0.29	0.64	0.72	0.39	0.39	0.42	0.15	0.21	0.35	0.43
Al_2O_3	7.54	8.24	9.79	8.03	6.09	11.24	12.51	6.70	6.74	6.20	2.92	4.45	7.3	9.4
FeO	ND	ND	0.84	0.74	1.67	2.97	5.90	2.32	2.57	1.90	ND	4.35	ND	ND
Fe_2O_3	7.00*	9.14*	14.01	11.21	2.43	5.10	3.30	4.92	4.57	3.34	11.63*	2.14	4.6*	6.2*
MnO	2.89	4.72	3.44	5.47	2.25	5.60	3.12	10.62	10.88	10.54	21.36	16.03	13	22
MgO	1.73	1.81	1.12	1.26	0.97	5.02	3.08	2.80	2.73	2.60	2.23	0.98	0.4	2.0
CaO	0.73	0.67	0.94	0.95	0.42	7.00	5.90	1.44	1.48	3.88	7.01	8.82	1.9	4.2
Na_2O	0.20	0.20	2.92	2.60	0.03	1.94	1.61	1.18	1.17	0.21	0.10	0.20	0.14	0.17
K_2O	1.78	1.66	1.78	0.86	1.36	0.80	0.76	0.39	0.38	0.96	0.01	0.02	0.1	0.31
P_2O_5	0.10	0.21	0.33	0.19	0.15	0.08	0.26	0.22	0.21	0.26	0.59	0.30	0.05	0.10
H_2O^-	ND	ND	0.08	0.01	0.01	0.33	0.26	0.03	0.06	0.22	ND	ND	ND	ND
CO_2	ND	ND	0.37	0.26	0.07	0.09	0.11	0.06	0.11	0.29	ND	0.66	ND	ND
LOI.	0.79	1.42	1.44	1.34	1.44	1.55	1.07	0.39	0.48	0.52	0.84	ND	2.0	3.1
Total	100.04	100.15	99.68	99.63	99.72	99.47	99.72	100.04	100.00	99.91	97.99	99.95	ND	ND
Rb	59	49	40	18	26	8	45	5	6	28	0.3	3	4.7	4.4
Sr	16	25	228	176	19	345	150	120	120	95	45	35	53	155
Ba	640	1200	1090	72	1030	1000	1330	473	486	834	40	917	24	1840
Y	11	19	22	25	14	18	35	20	21	24	28	23	ND	ND
Zr	74	100	88	87	52	48	120	62	59	82	27	41	57	94
Nb	8	7	6	6	–	–	9	7	7	11	3	8	53	63
Co	3	16	24	49	63	160	73	32	26	29	44	40	ND	ND
Sc	14	13	18	23	10	28	17	13	10	14	ND	7.6	ND	ND
Cr	41	42	46	42	54	44	47	50	52	81	51	59	44	68
V	45	67	73	36	48	–	93	27	26	59	52	270	ND	ND
Ni	84	89	73	80	91	125	78	53	45	73	ND	60	ND	ND
Zn	100	190	80	80	100	90	61	84	80	68	100	79	ND	ND
Pb	15	15	10	9	15	8	8	6.9	8	5.2	1.8	1.5	32	32
Cu	110	35	ND	ND	ND	ND	ND	5.8	11	30	ND	35	ND	ND
Sn	2.4	1.7	ND	ND	ND	ND	ND	2.1	3.7	2.7	0.26	1.5	ND	ND
La	14	23	ND	ND	ND	ND	ND	11	12	19	35	21	ND	ND
Ce	42	66	ND	ND	ND	ND	ND	26	24	56	63	61	ND	ND
Pr	3.75	5.92	ND	ND	ND	ND	ND	2.72	2.47	4.48	5.87	4.79	ND	ND
Nd	15	23	ND	ND	ND	ND	ND	10	9	16	21	20	ND	ND
Sm	3.24	5.48	ND	ND	ND	ND	ND	2.70	2.50	3.74	4.36	4.68	ND	ND
Eu	0.6	0.96	ND	ND	ND	ND	ND	0.62	0.56	0.86	0.81	1.09	ND	ND
Gd	2.73	4.81	ND	ND	ND	ND	ND	2.82	2.64	3.52	4.50	4.71	ND	ND
Tb	0.47	0.79	ND	ND	ND	ND	ND	0.45	0.44	0.53	0.66	0.72	ND	ND
Dy	2.84	4.75	ND	ND	ND	ND	ND	2.84	2.64	3.06	3.94	4.08	ND	ND
Ho	0.59	1.18	ND	ND	ND	ND	ND	0.59	0.55	0.65	0.83	0.88	ND	ND
Er	1.64	3.26	ND	ND	ND	ND	ND	1.53	1.48	1.66	2.16	2.40	ND	ND
Tm	0.24	0.45	ND	ND	ND	ND	ND	0.23	0.22	0.25	0.29	0.32	ND	ND
Yb	1.38	2.42	ND	ND	ND	ND	ND	1.36	1.35	1.57	1.58	1.79	ND	ND
Lu	0.21	0.42	ND	ND	ND	ND	ND	0.22	0.21	0.25	0.23	0.26	ND	ND
Th	5.84	7.37	ND	ND	ND	ND	ND	2.17	2.04	3.78	1.47	5.12	2.3	3.7
U	1.12	1.47	ND	ND	ND	ND	ND	0.31	0.29	0.68	2.11	3.26	ND	ND
Cs	3.59	2.28	ND	ND	ND	ND	ND	0.35	0.34	0.58	0.02	0.40	ND	ND

Note. BR, BRL, gondites and manganic quartzites of Almarnatol occurrence (I) (section of the Burlya River), US, UST, gondites of the Usutai deposit (II) (Usutai River). Dash, the element content is below the detection level, Fe_2O_3*, all iron is in the Fe^{3+} form. Sample SE 1165A is from E.V. Sklyarov's collection (Olkhon terrane), petrogenic elements were detected by XFA method (analyst G.V. Pashkova) and rare earth elements were determined by ICP MS method at the Geodynamics and Geochronology CUC. Sample MH-130 is from L.Z. Reznitsky's collection (Khamar-Daban terrane). 1, pure gondites; 2, multimineral gondites (medium content determined in accord with (Melcher, 1995).
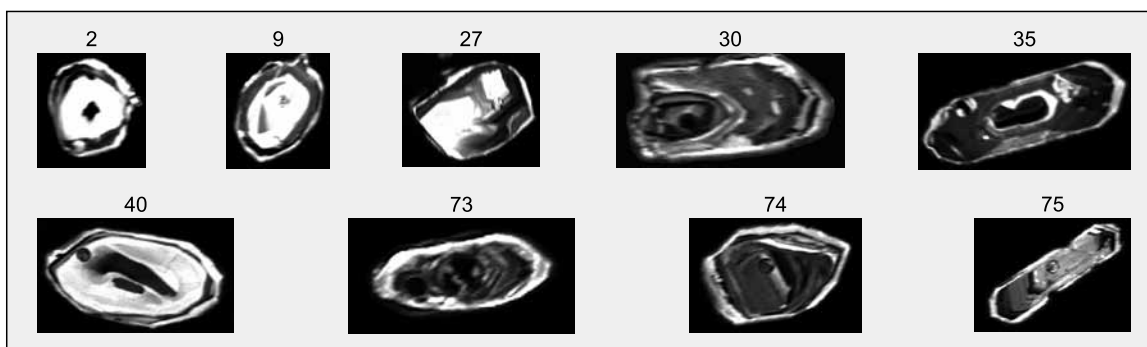
Fig. 11. Examples of zircons crystals from gneiss of the Itantsa Formation (cathodoluminescent photo). Zircons numbers correspond to analyses results in Table 4.

figurative points position of Mn-bearing rocks compositions on $Na_2O + K_2O–SiO_2/10–CaO + MgO$ diagram (Taylor and McLennan, 1985) (Fig. 13) illustrates that the evident differences of petrochemical manganese rocks composition are due to the presence of various sources of the volcaniclastic material being the main one for the cross-sectional part of the Usutai deposit rocks and for the acidic rocks of the Almarnatol occurrence. Flattening of REE curves and the decrease of Eu anomaly value in gondites from the Usutai deposit are the consequences of the increased volcaniclastic material content in their composition.

Recognition of hydrogenous and hydrothermal sources of substances in Mn-bearing deposits is based on both mineralogical and geochemical features of the composition. Hydrogenous Fe–Mn deposits tend to distribute in the regions where active volcanism occurrences are not observed; and typomorphic microelements peculiar to these deposits are: Co, Ni, Mo, Y, Th and REE (Flohr and Huebner, 1992; Dubinin et al., 2008; etc.). Formation of hydrothermal Fe-Mn deposits is controlled by the discharge zones of hydrothermal solutions in the volcanically active areas. The main geochemical criteria are considered to be low concentrations of

rare and rare earth elements (Anikeeva et al., 2008; Dubinin et al., 2008; etc.). With the use of Co–Zn–Ni deposits partition diagrams into hydrothermal and hydrogenous (Cronan, 1980) (Figs. 14, 15), we can come to conclusion that the main source of ore sediments was hydrothermal in nature. The signs of hydrothermal provenance in certain samples are as follows: high concentrations of Co, Ce and the total amount of REE. At the same time, the considerable contribution of the volcanoterrigenous component in the composition of the sedimentary deposit is estimated by close to PAAS, microelement REE spectra in the Mn-bearing rocks. We have to conclude that the differences in chemical composition of manganese rocks of the Itantsa Formation are predetermined by the variations of contribution, such as volcanoterrigenous, hydrothermal, and probably hydrogenous sources. They are certain to define the various protolith composition and the following postsedimentation changes resulted in significant transformations in the mineral composition of the formations under study.

Mineral manganese associations in Northern Ghana (Melcher, 1995) are represented by wide rocks spectra, i.e., from garnet-containing chlorite shale to pure and multimin-
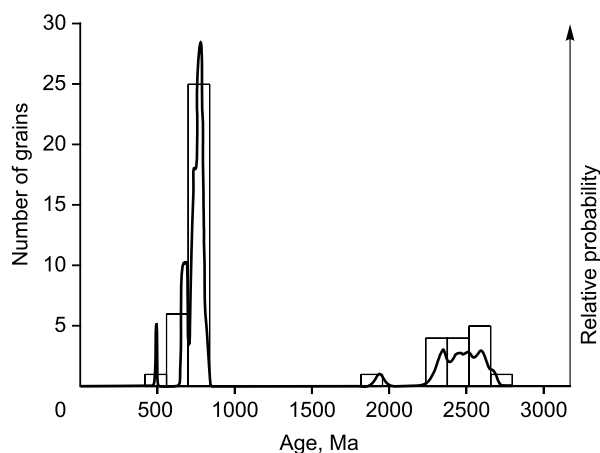
Fig. 12. Histogram (U–Pb (< 1 Ga) and Pb–Pb (> 1 Ga)) and the curve of relative probability of ages for detrital zircons from gneisses of the Itantsa Formation.
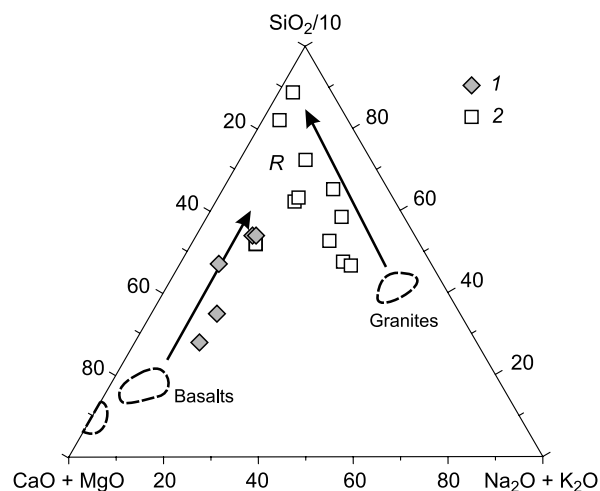
Fig. 13. Diagram $Na_2O + K_2O–SiO_2/10–CaO + MgO$ (Taylor and McLennan, 1985) for manganese rocks of the Itantsa Formation. *1*, Usutai deposit; *2*, Almarnatol occurrence. *R*, trend of destruction of acidic and basic rocks. See Fig. 8 for designations.
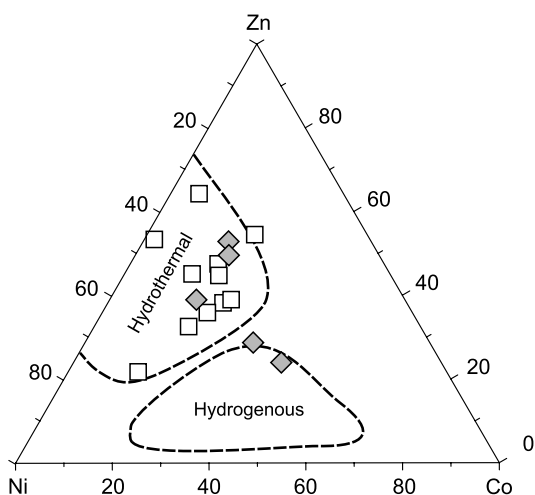
Fig. 14. Diagram Co–Zn–Ni (Cronan, 1980) for manganese rocks of the Itantsa Formation. See Fig. 8 for designations.

eral gondites (Fig. 4). Garnet composition of these associations is controlled by bulk rocks composition and is confined to the conditions of manganese deposits formation and, in particular, to the remoteness factor from the zones of thermal springs discharge. The garnets from the Itantsa Formation fall into two groups: the 1st group (the garnets from the Almarnatol occurrence) is located in the field of distal deposits (pure gondites in accord with (Melcher, 1995)); the 2nd group is related to proximal deposits (multimineral gondites) and mostly represented by the garnets from the Usutai deposit and partially from the Almarnatol occurrence. The compositions of garnets from the Slyudyanka and Olkhon terranes (Koneva, 2003) are introduced for comparison; they tend to concentrate mainly in the field of the 2nd group rocks. Depending on the total/gross Mn content in the rock, it would be difficult to define the conditions of the rock's formation. For instance, the garnets of spessartine series appear to be stable within a wide range of metamorphic transformations—from the lowest greenschist facies (400 °C, 2 kbar (Hsu, 1968)) up to granulite; which is why it is not advisable to use them for P–T-parameters estimation. The composition of the manganese amphibole also depends on the chemical composition of the host rocks. Under conditions of high-temperature metamorphism (the upper amphibolite facie), Mn-amphibole is of rare occurrence for

most Mn–Mg–Fe host rocks (Melcher, 1995), it is more typical for low-temperature conditions (Dasgupta, 1985; Melcher, 1995). Manganese cummingtonite (tirodite) with the composition (Mn/(Mn + Mg) = 0–0.3) is stable at low pressures (2 kbar) in the temperature ranges of 400–620 °C and 570– 750 °C (Melcher, 1995). According to (Dasgupta et al., 1985) (Fig. 16) Mn-cummingtonite can be stable at pressure of 3 kbar and at the temperature of 580 to 640 °C, and in association with Mn-pyroxene it remains stable at higher parameters. In the sequence of Pribaikalia, the rocks of the gondite formation (as mentioned above) were studied within the borders of the Olkhon and the Khamar-Daban terranes, which are distinguished by high degree of metamorphic alterations. Both P–T conditions in the zone of gondites distribution within the Olkhon terrane (Table 5) and the composition of Mn-cummingtonite detected only in the rocks of the Olkhon terrane are close to the metamorphism parameters of Sausar and Tirodi Formations (Dasgupta et al., 1988). Similar mineral associations and the compositions of Mn-cummingtonite from the Usutai deposit and the gondites from the Nangodi belt (Northern Ghana) make us assume that the rocks formation took place under conditions with close or congruent parameters (Table 5). The level of metamorphism supposedly was bit lower (might have been at the level of 400–450 °C) in the zone of gondites propagation within the Almarnatol occurrence.

In accordance with the findings of the geochronological studies, the main provenance areas for the terrigenous rocks of the Itantsa Formation are found to be early Paleoproterozoic–Neoarchean (2670–2312 Ma) and early Neoproterozoic (812–717 Ma) formations. Detrital zircons with the age interval of 700–850 Ma are common for most terranes formations southwards within the structure of the adjacent Siberian platform: Khamar-Daban, Ikat, Tunka, and Dzhida terranes (Kovach et al., 2013; Reznitsky et al., 2013, 2015a,b; Shkol'nik et al., 2016; etc.). Magmatic formations of different geodynamic nature of the early Neoproterozoic are characterized by wide propagation area within the eastern segment of Central Asian fold belt (CAFB) (Kuzmichev et al., 2001, 2005; Levashova et al., 2010; Kuzmichev and Larionov, 2011; Rytsk et al., 2011, 2013; Kozakov et al., 2014; Orsoev et al., 2015; etc.). The wide distribution area of Neoproterozoic formations makes the unique definition of the provenance area rather complicated for the terrige-

Table 5. Sm–Nd isotopic data for manganese rocks of the Itantsa Formation

Sample No.	T, Ma	Content, ppm		^{147}Sm/^{144}Nd	^{143}Nd/^{144}Nd $\pm 2\sigma$	$\varepsilon_{Nd}(0)$	$\varepsilon_{Nd}(T)$	$T_{Nd}(C)$
		Sm	Nd					
US-1	500	2.70	10.25	0.1586	0.152054 ± 11	−11.4	−9.0	1.9
US-7	500	2.50	9.62	0.1564	0.511997 ± 14	−12.9	−10.3	2.0
BR-23*	500	3.01	14.69	0.1238	0.511928	−13.8	−9.2	2.0
BR-25*	500	4.25	20.66	0.1244	0.511983	−12.8	−8.2	1.9

Note. Values $\varepsilon_{Nd}(T)$ and two-stage model ages $T_{Nd}(C)$ computed for minimum possible accumulation age.
*From (Letnikova et al., 2016).
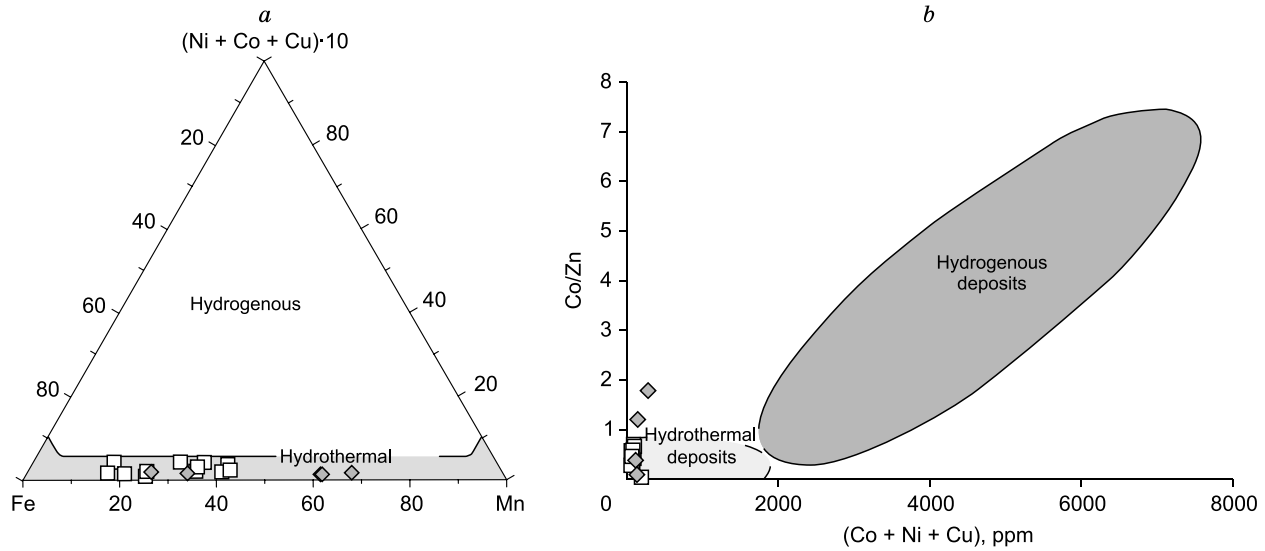
Fig. 15. Diagrams Mn–(Ni + Co + Cu)*–Fe (*a*) (Bonatti et al., 1972) and Co + Ni + Cu–Co/Zn (*b*) (Toth, 1980) for manganese rocks of the Itantsa Formation. See Fig. 8 for designations.

nous formation rocks. According to Nd-isotope data (Rytsk et al., 2011), the ancient early Proterozoic continental crust is situated on the base of the stratified sections of the Barguzin–Vitim (Ikat) terranes. The data obtained on detrital zircons give evidence in support of the fact that the dominating provenance area was the early Paleoproterozoic (2.46–2.31) and Neoarchean (2.67–2.51) rocks. The Siberian Craton with its broad development within the limits of the 1.9–1.8 Ga age interval and the absence of early Paleoproterozoic formations cannot be considered as a source-land. Geochronological data on cratonic terranes of the CAFB are rather scarce, and such duplication of age intervals is absolutely atypical. The data obtained on the provenance area are consistent with the conclusion made by E.Yu. Rytsk (Rytsk et al., 2011) about the inaccessibility or isolation of the Barguzin–Vitim terrane paleostructures from the Siberian Craton. In view of this, it is supposed that the existence of the ancient continental block within the current Ikat terrane does not have any connection with the Siberian Craton and it is completely overlaid with volcanosedimentary formations and younger age granitoids from the Angara–Vitim batholith. The minimum age peak of the detrital zircons complies with the point of 660 Ma. The events in the age interval of 690–665 Ma are not widely distributed within the east segment of CAFB. Detrital zircons of this time interval are found only in terrigenous rocks of the Dzhida and Khamar-Daban terranes (Reznitsky et al., 2013; Shkol'nik et al., 2016); they are also the most characteristic for the magmatic complexes of the eastern Transbaikalia CAFB segment (Rytsk et al., 2011). This age interval is likely to be in compliance with the time of the Mn-occurrences being synchronous with the sedimentation process and manganese accumulations with basite magmatism of the Itantsa Formation. The most significant result of the Itantsa Formation de-

trital zircons study is the absence of the 1000–850 Ma age interval in the zircons provenance area despite the fact that this time span is the most typical for the Transbaikalia branch of the fold belt (Nekrasov et al., 2007; Ruzhentsev et al., 2007, 2012; Rytsk et al., 2011; etc.).

The geological position of the above-mentioned manganese occurrences in the northeast part of the CAFB is determined by their assignment to the Vendian–Cambrian volcanosedimentary sequences, whose formation took place within the active continental margin in the setting of the back-arc basin (Makrygina et al., 2000; Reznitsky et al.,
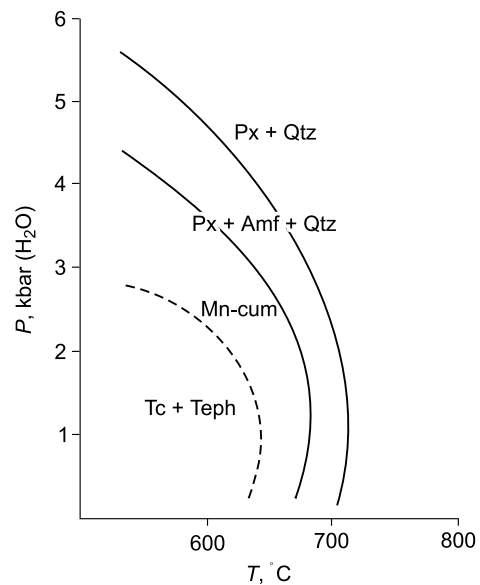
Fig. 16. *P–T* diagram of stability for Mn-cummingtonite (Dasgupta, 1985). Fields of stability for associations: Tc + Teph, talc + tephroite; Mn-cum, Mn-cummingtonite; Px + Amf + Qtz, pyroxene + amphibole + quartz, Px + Qtz, pyroxene + quartz.

Table 6. U–Pb isotopic data on zircons from gneisses of the Itantsa Formation

No. point of analysis	Isotope relations						Rho	Age, Ma						D, %
	$^{207}Pb/^{206}Pb$	1σ	$^{207}Pb/^{235}U$	1σ	$^{206}Pb/^{238}U$	1σ		$^{207}Pb/^{206}Pb$	1σ	$^{207}Pb/^{235}U$	1σ	$^{206}Pb/^{238}U$	1σ	
3	0.06463	0.0010	1.05022	0.0163	0.11796	0.0011	0.63	762.2	34.51	729	8.1	718.8	6.66	−5.69
4	0.06388	0.0012	0.95636	0.0176	0.10868	0.0011	0.56	737.7	40.64	681.4	9.16	665.1	6.51	−9.84
5	0.16021	0.0024	9.59483	0.1378	0.43475	0.0047	0.76	2457.9	25.33	2396.7	13.21	2327.1	21.31	−5.32
7	0.11879	0.0017	5.45190	0.0759	0.33323	0.0034	0.73	1938.1	26.26	1893.1	11.96	1854	16.49	−4.33
8	0.06669	0.0011	1.15302	0.0191	0.12555	0.0012	0.61	828	36.12	778.7	9.01	762.4	7.23	−7.92
9	0.16630	0.0030	10.87031	0.1920	0.47464	0.0060	0.72	2520.8	30.18	2512.1	16.43	2503.9	26.36	−0.67
11	0.06283	0.0019	1.05242	0.0308	0.12166	0.0015	0.44	702.3	63.36	730.1	15.24	740.1	8.89	5.38
15	0.06189	0.0009	0.92535	0.0136	0.1086	0.0010	0.66	670.3	33.21	665.2	7.22	664.6	6.14	−0.85
17	0.15619	0.0019	9.27772	0.1042	0.43147	0.0040	0.83	2414.9	20.43	2365.8	10.3	2312.3	18.12	−4.24
18	0.15133	0.0019	8.23851	0.0973	0.39546	0.0037	0.81	2361	21.46	2257.6	10.69	2148.1	17.42	−9.01
20	0.06613	0.0011	1.12300	0.0186	0.12335	0.0012	0.61	810.6	36.07	764.4	8.9	749.8	7.16	−7.50
23	0.06351	0.0011	1.15024	0.0198	0.13158	0.0013	0.59	725.3	37.92	777.4	9.37	796.9	7.67	9.87
25	0.17465	0.0022	10.99412	0.1357	0.45733	0.0044	0.78	2602.7	21.71	2522.6	11.49	2427.8	19.46	−6.71
27	0.06707	0.0017	1.18432	0.0292	0.1283	0.0015	0.48	839.9	52.54	793.3	13.6	778.1	8.71	−7.35
29	0.18199	0.0026	11.81183	0.1660	0.47157	0.0048	0.73	2671.1	24.18	2589.6	13.16	2490.4	21.33	−6.76
30	0.16506	0.0023	9.76694	0.1296	0.42991	0.0042	0.74	2508.2	23.34	2413	12.22	2305.3	19.03	−8.08
35	0.06553	0.0014	1.16536	0.0248	0.12921	0.0014	0.52	791.5	45.75	784.5	11.64	783.3	8.15	−1.03
37	0.06398	0.0017	1.04754	0.0277	0.11896	0.0014	0.46	741	57	727.7	13.78	724.6	8.32	−2.21
38	0.06579	0.0014	1.13182	0.0239	0.12499	0.0013	0.52	799.8	45.3	768.6	11.4	759.2	7.91	−5.07
39	0.0564	0.0013	0.61461	0.0144	0.07917	0.0008	0.48	467.5	53.68	486.5	9.11	491.2	5.31	5.06
40	0.16007	0.0025	10.02731	0.1538	0.45517	0.0046	0.67	2456.4	26.68	2437.3	14.16	2418.2	20.67	−1.55
47	0.1504	0.0026	8.36687	0.1421	0.40419	0.0042	0.62	2350.5	29.6	2271.6	15.41	2188.3	19.4	−6.90
48	0.14707	0.0025	7.97314	0.1320	0.39388	0.0040	0.61	2312.2	29	2228	14.94	2140.8	18.52	−7.41
49	0.06776	0.0016	1.19167	0.0274	0.12777	0.0014	0.5	861.3	48.58	796.7	12.73	775.1	8.36	−10.0
52	0.06536	0.0015	1.13478	0.0261	0.12615	0.0014	0.49	785.8	48.95	770	12.43	765.9	8.21	−2.53
53	0.06395	0.0015	1.06398	0.0245	0.12088	0.0013	0.49	739.9	49.32	735.8	12.06	735.6	7.89	−0.58
60	0.06501	0.0016	1.07685	0.0266	0.12034	0.0014	0.47	774.6	52.36	742.1	13.02	732.5	8.09	−5.43
64	0.06245	0.0018	1.01183	0.0298	0.1177	0.0014	0.43	689.5	63.04	709.8	15.06	717.3	8.62	4.03
65	0.17321	0.0037	11.16882	0.2396	0.46842	0.0052	0.52	2588.9	35.83	2537.3	19.99	2476.6	22.96	−4.33
71	0.06513	0.0021	1.08926	0.0353	0.12149	0.0016	0.41	778.5	68.11	748.1	17.19	739.1	9.4	−5.06
73	0.0631	0.0017	0.96738	0.0263	0.11136	0.0013	0.44	711.6	57.63	687.1	13.6	680.7	7.8	−4.34
74	0.17002	0.0042	10.93989	0.2727	0.4674	0.0056	0.48	2557.8	41.42	2518	23.19	2472.2	24.73	−3.34
75	0.06424	0.0021	1.00496	0.0331	0.11364	0.0015	0.41	749.5	69.43	706.3	16.79	693.8	8.88	−7.43
78	0.06768	0.0019	1.17946	0.0343	0.12658	0.0015	0.43	858.8	59.98	791.1	16	768.3	9.08	−10.5
79	0.06666	0.0019	1.14416	0.0337	0.12467	0.0015	0.43	827.2	60.97	774.5	15.97	757.4	9.01	−8.43
82	0.06485	0.0025	1.15308	0.0450	0.12915	0.0019	0.39	769.5	81.55	778.7	21.25	783	11.14	1.75
84	0.17376	0.0049	10.34696	0.2916	0.43251	0.0053	0.44	2594.2	46.39	2466.3	26.1	2317	24.22	−10.6
89	0.06934	0.0023	1.28282	0.0427	0.13437	0.0018	0.4	908.9	67.6	838.1	18.99	812.7	10.28	−10.5
93	0.06526	0.0023	1.12035	0.0396	0.12469	0.0017	0.39	782.6	73.2	763.1	19	757.5	9.92	−3.20
95	0.06625	0.0022	1.16827	0.0396	0.12808	0.0017	0.4	814.2	69.69	785.8	18.58	776.9	9.85	−4.58
96	0.0638	0.0023	1.12459	0.0416	0.12802	0.0018	0.38	735	76.94	765.2	19.89	776.6	10.4	5.65
98	0.06538	0.0026	1.14904	0.0453	0.12763	0.0019	0.38	786.7	81.36	776.8	21.41	774.3	10.89	−1.57
104	0.15246	0.0057	8.40083	0.3141	0.40017	0.0058	0.39	2373.7	62.42	2275.3	33.93	2169.8	26.84	−8.58

Table 7. Mineralogical and metamorphic parameters of tirodite-containing associations

Position Mn-containing rocks	X_{Mg} Amp	X_{Mn} Amp	Mineral associations	T, ˚C	P, kbar	Reference
Ikat terrane (Usutai deposit)	0.78–0.79	0.28–0.30	Grt + Pft + Rdn + Qtz	500–550	2–3	Present study
Olkhon terrane	0.99	0.37	Grt + Pxm + Px (Fe–Mg–Mn–Ca series) + Cam	600	6.5–8.5	(Koneva et al., 1998) (Petrova and Levitsky, 1984)
Tirodi	1.0	0.12	Grt + Rdn	650±25	6	(Dasgupta et al., 1988)
Sausar Formation	0.95–0.99	0.30–0.36	Grt + Pxm ± Rdc	600	6	(Dasgupta et al., 1988)
Nangodi Belt (Northern Ghana)	0.58–0.77	0.20–0.34	Grt + Cam + Rdn + Stilp + Qtz	450–500	2–3	(Melcher, 1995)
Nigeria	0.50–0.75	0.11–0.21	Grt + Cam + Rdc + Ilm	540–610		(Neumann, 1988)

Note. Grt, garnet; Pft, pyrophanite; Ilm, ilmenite; Rdn, rhodonite; Pxm, pyroxmangite; Px, pyroxene; Cam, Ca amphibole; Rdc, rhodochrosite; Stilp, stilpnomelane; Qtz, quartz.

2004; Belichenko et al., 2006, Gordienko et al., 2010; etc.). Present-day hydrothermal-hydrogenous Fe-Mn-bearing crusts with different chemical compositions predominantly tend to locate in the transitional zone from the continent to the ocean, which is characterized by high volcanic activity. The most perfect example of both Mn-occurrences and deposits formation within the arc–back-arc basin system is recognized to be the Western Pacific transitional area (Usui and Soweya, 1997; Davidov, 2004, Anikeeva et al., 2008; etc.). Regarding the genesis of both current and ancient manganese deposits, it will be important to define not only the sources of manganese transport, but the conditions of feasible deposition of this metal. If iron is removed from the oceanic ore genesis into the sedimentary unit under both acidizing and reduction conditions, manganese could stay in solid-phase form only in oxidized conditions (Bazilevskaya, 2006). Herewith, the most favorable conditions of manganese accumulation are certain to be both in the marginal-continental sedimentary basin and in the volcanosedimentary basin, which are distinguished by submarine character of terrigenous-carbonate deposits and by vigorous exhalative-hydrothermal activity. Hydrothermal iron-manganese deposits are genetically bound to the regions of volcanic activity occurrences which are characterized by tectonic settings like: mid-oceanic rifts, island arcs and back-arc basins. Being close in mineral and geochemical composition, the gondite association rocks of the Ikat, Olkhon, and Khamar-Daban terranes were likely to form within the borders of a single lengthy marginal basin with evident volcanic activity and favorable conditions for manganese accumulation.

CONCLUSIONS

According to the obtained isotope-geochemical and mineralogical data we conclude that the formation of the carbonate–effusive–shale complex of the Itantsa Formation corresponds to manganese mineralization and took place in the sedimentary basin located in the nearest proximity to the continental provenance area under conditions of volcanic activity being synchronous to sedimentation process. In ac-

cord with the available data set, manganese deposits could fall into distal (remote from the center of exhalative-hydrothermal activity) and proximal types. The difference of chemical and mineral compositions of two manganese deposits of the Itantsa Formation is associated with various sources of material, the degree of proximity to the mouths of hydrothermal activity, and also by different extent of post-sedimentary alterations. Accumulation of Mn-bearing formation deposits was detected in the late Neoproterozoic (Ediacaran) rocks within the borders of the active margin of the ancient late Paleoproterozoic continental block. Accumulation of Mn-bearing deposits occurred on the territory of the Central Asian fold belt and within the borders of the Khamar-Daban and Olkhon terranes and probably within a single system of back-arc basins.

REFERENCES

Anikeeva, L.I., Kazakova, V.E., Gavrilenko, G.M., Rashidov, V.A., 2008. Ferrous-manganese crustal formations of the West Pacific transitional zone. Vestnik KRAUNTs, Nauki o Zemle 11 (1), 10–31.

Bazilevskaya, E.S., 2006. Sources of manganese deposited as oceanic Fe–Mn ore. Geology of Ore Deposits 48 (2), 134–143.

Belichenko, V.G., 1969. The Lower Paleozoic of Western Transbaikalia [in Russian]. Nauka, Moscow.

Belichenko, V.G., Geletii, N.K., Barash, I.G., 2006. The Bargusin microcontinent: on the problem of separation. Russian Geology and Geophysics (Geologiya i Geofizika) (10), (1049–1059).

Betekhtin, A.G., 1946. Production Manganese Ores of the USSR [in Russian]. Leningrad.

Bonatti, E., Kraemer, T., Rydell, H., 1972. Classification and genesis of submarine iron-manganese deposits, in: Horn, D. (Ed.), Ferromanganese Deposits on the Ocean Floor. Int. Decade on Ocean Exploration, pp. 149–161.

Boström, K., 1974. Origin and Fate of Ferromanganoan Active Ridge Sediments. Pelagic Sediments. Land and Sea. Oxford.

Bowles, J.F.W., Howie, R.A., Vaughan, D.J., Zussman, J., 2011. Rock-Forming Minerals. Vol. 5A. Nonsilicates: Oxides, Hydrooxides and sulfides. Geol. Soc., London.

Brusnitsyn, A.I., 2015. The Parnok Manganese Deposit, the Polar Urals: Mineralogy, Geochemistry, and Ores Genesis [in Russian]. St.-Petersburg. Gos. Univ., St.-Petersburg.

Butuzova, G.Yu., 1998. Hydrothermal Sedimentary Ore-Formation in the Rift Zone of the Red Sea [in Russian]. GEOC, Moscow.

Cronan, D.S., 1980. Underwater Minerals. Academic Press, London.

Czamanske, G.K., Mihailik, P., 1972. Oxidation during magmatic differentiation, Finnmarka Complex, Oslo area, Norway. Pt. 1: The opaque oxides. J. Petrol. 13, 493–509.

Dasgupta, S., Miura, H., Hariya, Y., 1985. Stability of Mn-cummingtonite–an experimental study. Mineral. J. 12, 251–259.

Dasgupta, S., Bhattacharya, P.K., Chattopadhyay, G., Banerjee, H., Majimdar, N., Fukuoka, M., Roy, S., 1988. Petrology of Mg–Mn amphibole-bearing assemblages in manganese silicate rocks of the Sausar Group, India. Mineral. Mag. 52, 105–111.

Dasgupta, S., Banerjee, H., Fukuoka, M., Bhattacharya, P.K., Roy, S., 1990. Petrogenesis of metamorphosed manganese deposits and the nature of precursor sediments. Ore Geol. Rev. 5, 359–384.

Davidov, M.P., 2004. Geochemistry of Fe–Mn deposits of the rift zone of the northern pre-equatorial section of the MAR—a comparative study, in: Minerals of the Ocean—Integrated Strategies-2. Conf. Abstracts. St.-Petersburg: VNIIOkeangeologia, pp. 129–130.

Deer, W., Howie, R.A., Zussman, J., 1963. Rock-Forming Minerals, Vol. 5: Non-Silicates. Longmans, London.

Dubinin, A.V., Uspenskaya, T.Yu., Gavrilenko, G.M., Rashidov, V.A., 2008. Geochemistry and genesis of Fe–Mn mineralization in island arcs in the West Pacific Ocean. Geochem. Int. 46 (12), 1206–1227.

Fermor, L.L., 1909. The Manganese Ore deposits of India. Mem. Geol. Surv. India. Vol. 37.

Flohr, M.J.K., Huebner, J.S., 1992. Mineralogy and geochemistry of two metamorphosed sedimentary manganese deposits, Sierra Nevada, California, USA. Lithos 29, 57–85.

Golovko, V.A., Ikonnikova, Z.I., 1977. Gondites of the Western Sayans [in Russian]. VINIITI, Moscow.

Golovko, V.A., Mstislavskii, M.M., Nasedkina, V.Kh., 1982. Pre-Cambrian manganese bearing capacity of the Yenisei Ridge, in: Manganese Geology and Geochemistry [in Russian]. Nauka, Moscow, pp. 94–104.

Gordienko, I.V., Bulgatov, A.N., Ruzhentsev, S.V., Minina, O.R., Klimuk, V.S., Vetluzhskikh, L.I., Nekrasov, G.E., Lastochkin, N.I., Sitnikova, V.S., Metelkin, D.V., Goneger, T.A., Lepekhina, E.N., 2010. The Late Riphean–Paleozoic history of the Uda–Vitim island arc system in the Transbaikalian sector of the Paleoasian ocean. Russian Geology and Geophysics (Geologiya i Geofizika) 51 (5), 461–481 (589–614).

Gurvich, E.G., 1998. Metal-Bearing Sedimentary Deposits of the World Ocean [in Russian]. Nauchnyi Mir, Moscow.

Gurvich, E.M., Gribov, E.M., Rakhmanov, V.P., 1982. Pre-Cambrian carbon-containing manganese-bearing formation, in: Manganese Geology and Geochemistry [in Russian]. Nauka, Moscow, pp. 47–59.

Gusev, Yu.P., Osokin P.V., Zdarov, V.I., 1970. On the lithology and manganese-bearing potential of the Upper Proterozoic Itantsa Formation of the Morskoi Ridge (Southwest Pribaikalia), in: Trans. Geol. Depart. Buryat. Branch SB AS USSR, Issue 2 (10), pp. 19–27.

Hsu, L.C., 1968. Selected phase relationship in the system Al–Mn–Fe–Si–O–H: A model for garnet equilibria. J. Petrol. 9, 40–63.

Khubanov, V.B., Buyantuev, M.D., Tsygakov, A.A., 2016. U–Pb dating of zircons from PZ$_3$–MZ igneous complexes of Transbaikalia by sector-field mass spectrometry with laser sampling: technique and comparison with SHRIMP. Russian Geology and Geophysics (Geologiya i Geofizika) 57 (1), 190–205 (241–258).

Koneva, A.A., 2003. Mn–Fe–Mg rhomboidal pyroxene from gondite formation of Priolkhon'ye (Western Pribaikalia). Zapiski VMO, No. 6, 60–63.

Koneva, A.A., Makrygina, V.A., Piskunova, L.F., Ushchapovskaya, Z.F., 1991. On gondite association in Priolkhon'ye (Western Pribaikalia). Dokl. AN SSSR 319 (1), 213–218.

Koneva, A.A., Makrygina, V.A., Reznitsky, L.Z., 1998. Gondites in metamorphic thicknesses of the Pribaikalia. Litologiya i Poleznye Iskopaemye, No. 1, 93–102.

Kovach, V., Salnikova, E., Wang, K.-L., Jahn, B.-M., Chiu, H.-Y., Reznitsky, L., Kotov, A., Iizuka, Y., Chung, S.-L., 2013. Zircon ages and Hf isotopic constraints on sources of clastic metasediments of the Slyudyanka high-grade complex, southeastern Siberia: Implication or continental growth and evolution of the Central Asian Orogenic Belt. J. Asian Earth Sci. 62, 18–36.

Kozakov, I.K., Kovach, V.P., Bibikova, E.V., Kirnozova, T.I., Lykhin, D.A., Plotkina, Yu.V., Tolmacheva, E.V., Fuzgan, M.M., Erdenezhargal, Ch., 2014. Late Riphean episode in the formation of crystalline rock complexes in the Dzabkhan microcontinent: Geological, geochronologic, and Nd isotopic-geochemical data. Petrology 22 (5), 480–506.

Kuleshov, V.N., 2011. Manganese deposits. Communication 2: Major epochs and phases of manganese accumulation in the Earth's history. Lithol. Miner. Resour. 46 (6), 546–565.

Kulish, L.I., 1973. Manganese complexes of the Precambrian Far East, in: Lithology and Sedimentary Mineral Resources of the Precambrian Siberia and the Far East [in Russian]. SNIIGiMS, Novosibirsk, pp. 132–136.

Kuzmichev, A.B., Larionov, A.N., 2011. The Sarkhoi Group in East Sayan: Neoproterozoic (∼770–800 Ma) volcanic belt of the Andean type. Russian Geology and Geophysics (Geologiya i Geofizika) 52 (7), 685–700 (875–895).

Kuzmichev, A., Bibikova, E.B., Zhuravlev, D.Z., 2001. Neoproterozoic (800 Ma) orogeny in the Tuva-Mongolia Massif (Siberia): island arc–continent collision at the northeast Rodinia margin. Precambrian Res. 110, 109–126.

Kuzmichev, A., Kroner, A., Hegner, E., Liu D., Wan Yu., 2005. The Shishkhid ophiolite, northern Mongolia: A key to the reconstruction of a Neoproterozoic island-arc system in central Asia. Precambrian Res. 138, 125–150.

Letnikova, E.F., Letnikov, F.A., Shkol'nik, S.I., Cherkashina, T.Yu., Reznitsky, L.Z., Vishnevskaya, I.A., 2016. Nd isotope systematics of the Vendian–Early Cambrian sedimentary ores in the northern segment of the Paleoasian Ocean. Dokl. Earth Sci. 466 (1), 42–46.

Levashova, N.M., Kalygin, V.M., Gibsher, A.S., Yff, G., Ryabinin, A.B., Meert, J.G., Malone, S.J., 2010. The origin of the Baydaric microcontinent, Mongolia: constraints from paleomagnetism and geochronology. Tectonophysics 485, 306–320.

Makrygina, V.A., Petrova, Z.I., Gantimurova, T.P., 2000. Andesite magmatism and its place in geological history of the Ol'khon area (western Baikal region). Geochem. Int. 38 (12), 1161–1174.

Melcher, F., 1995. Genesis of chemical sediments in Birimian greenstone belts: evidence from gondites and related manganese-bearing rocks from northern Ghana. Mineral. Mag. 59, 229–251.

Mohaparta, B.K., Nayak, B., 2005. Petrology of Mn carbonate-silicate rocks from the Gangpur Group, India. J. Asian Earth Sci. 25. 773–780.

Nekrasov, G.E., Rodionov, N.V., Berezhnaya, N.G., Sergeev, S.A., Ruzhentsev, S.V., Minina, O.P., Golionko, B.G., 2007. U-Pb age of zircons from plagiogranite veins in migmatized amphibolites of the Shaman Range (Ikat–Bagdarin zone, Vitim Highland, Transbaikal region). Dokl. Earth Sci. 413 (1), 160–163.

Neumann, U., 1988. Mineralogie and genese der Manganvorkommen in den Schiefergürteln von Nord-Nigeria. PhD Thesis. Univ. Göttingen, Göttingen.

Orsoev, D.A., Mekhonoshin, A.C., Gordienko, I.V., Badmatsyrenova, R.A., Kanakin, S.V., Travin, A.V., Volkova, M.G., 2015. The Riphean Meteshikha island-arc peridotite-gabbro massif (western Transbaikalia). Russian Geology and Geophysics (Geologiya i Geofizika) 56 (9), 1213–1231 (1549–1571).

Osipenko, A.B., Sidorov, E.G., 1999. Pyrophanite, manganoilmenite and Mn-armalcolite from the hyperbasite massifs of Kamchatka. Zapiski VMO, No. 6, 68–73.

Osokin, P.V., Bulgatov, A.N., Kvashnin, V.G., 1989. Sedimentary-volcanogenic formations of the Morskoi Range (Transbaikal) and their minerogenesis. (Geologiya i Geofizika) (Russian Geology and Geophysics) 30 (5), 50–58 (45–52).

Panteeva, S.V., Gladkochoub, D.P., Donskaya, T.V., Markova, V.V., Sandimirova, G.P., 2003. Determination of 24 trace elements in felsic rocks by inductively coupled plasma mass spectrometry after lithium metaborate fusion. Spectrochim. Acta Part B: Atomic Spectroscopy 58 (2), 341–350.

Pin, C., Santos Zalduegui J.F., 1997. Sequential separation of light rare-earth elements, thorium and uranium by miniaturized extraction chromatography: Application to isotopic analyses of silicate rocks. Anal. Chim. Acta 339, 79–89.

Rakhmanov, V.P., Grigor'ev, V.M., Chaikovskii, V.K., 1982. Manganese-bearing provinces and manganese formations on the territory of the USSR, in: Manganese Geology and Geochemistry [in Russian]. Nauka, Moscow, pp. 5–14.

Reznitsky, L.Z., Vasil'ev, E.P., Vishnyakov, V.N., 1976. The first gondite find in the Pre-Cambrian Southern Pribaikalia. Dokl. AN SSSR 229 (5), 1195–1197.

Reznitsky, L.Z., Shkol'nik, S.I., Levitskii, V.I., 2004. Geochemistry of calcium-silicate rocks of the Kharagol Formation (South Pribaikalia). Litologiya i Poleznye Iskopayemye, No. 2, 1–14.

Reznitsky, L.Z., Kovach, V.P., Barash, I.G., 2013. Provenance areas of terrigenous rocks of the Dzhidinsky island-arc terrane: based on data on U–Pb LA-ICPMS dating of detrital zircons, in: Proc. Conf. "Geodynamic Lithosphere Evolution of the Central Asian Mobile Belt (from Ocean to Continent)" [in Russian]. IZK SO RAN, Irkutsk, pp. 194–195.

Reznitsky, L.Z., Shkol'nik, S.I., Ivanov, A.V., Demonterova, E.I., Letnikova, E.F., Hung, C.-H., Chung, S.-L., 2015a. The Hercynian Ikat thrust in the Transbaikalian segment of the Central Asian Orogenic Belt. Russian Geology and Geophysics (Geologiya i Geofizika) (12), 1671–1684 (2118–2133).

Reznitsky, L.Z., Demonterova, E.I., Barash, I.G., Hung, Ts.-Ch., Chung, S.L., 2015b. Lower age limit and provenance areas of metaterrigenous rocks of the allochthon of Tunka Bald Mountains (East Sayan). Dokl. Earth Sci. 461 (2), 356–359.

Roy, S., 1965. Comparative study of the metamorphosed manganese protores of the world. The problem of the nomenclature of the gondites and kodurites. Econ. Geol. 60, 1238–1260.

Ruzhentsev, S.V., Aristov, V.A., Minina, O.P., Golionko, B.G., Nekrasov, G.E., 2007. Hercynides of the Ikat-Bagdarin zone in Transbaikalia. Dokl. Earth Sci. 417 (1), 1198–1201.

Ruzhentsev, S.V., Minina, O.P., Nekrasov, G.E., Aristov, V.A., Golionko, B.G., Doronina, N.A., Lykhin, D.A., 2012. The Baikal-Vitim Fold System: Structure and geodynamic evolution. Geotectonics 46 (2), 87–110.

Rytsk, E.Yu., Kovach, V.P., Yarmolyuk, V.V., Kovalenko, V.I., Bogomolov, E.S., Kotov, A.B., 2011. Isotopic structure and evolution of the continental crust in the East Transbaikalian segment of the Central Asian Foldbelt. Geotectonics 45 (5): 349.

Rytsk, E.Yu., Kotov, A.B., Andreev, A.A., Yarmolyuk, V.V., Velikoslavinskii, S.D., Kovach, V.P., Makeev, A.F., Fedoseenko, A.M., 2013. The structure and age of the Baikal granitoid massif: New evidence for early Baikalian events in the Baikal-Muya mobile belt. Dokl. Earth Sci. 453 (2), 1205–1208.

Shkol'nik, S.I., Letnikova, E.F., 2015. Geochemistry of manganese ores from the southern folded margin of the Siberian platform. Geochem. Int. 53 (6), 545–553.

Shkol'nik, S.I., Stanevich, A.M., Reznitskii, L.Z., Savelieva, V.B., 2016. New data about structure and time of formation of the Khamar-Daban terrane: U-Pb LA-ICP-MS zircon ages. Stratigr. Geol. Corr. 24 (1), 19–38.

Shkol'nik, S.I., Reznitsky, L.Z., Barash, I.G., Levitskii, I.V., 2017. Gondites in the south fold belt structure of the adjacent Siberian Plate, in: Bychkov, I.V., Kazakov, A.L. (Eds.), Scientific Issues of the Pribaikalia. Issue 2 [in Russian]. IG SO RAN, Irkutsk, pp. 228–232.

Shkolnik, S.I., Letnikova, E.F., Maslov, A.V., Buyantuev, M.D., Reznitskii, L.Z., Barash, I.G., 2017. A Vendian manganese-bearing basin of the Ikat terrane: Formation settings and provenance areas. Dokl. Earth Sci. 475 (1), 739–742.

Snetsinger, K.G., 1969. Manganoan ilmenite from a Sierran adamellite. Am. Mineral. 54, 431–436.

Strakhov, N.M., 1976. The Geochemistry Issues of Contemporary Oceanic Lithogenesis [in Russian]. Nauka, Moscow.

Sun, S., McDonough, W.F., 1989. Chemical and isotopic systematics of oceanic basalts: implications for mantle composition and processes, in: Saunders A.D., Norry M.J. (Eds.), Magmatism in Oceanic Basins. Geol. Soc. London., Spec. Publ. 42, 313–345.

Taylor, S.R., McLennan, S.M., 1985. The Continental Crust: Its composition and evolution; an examination of the geochemical record preserved in sedimentary rocks. Blackwell, Oxford.

Toth, J.R., 1980. Deposition of submarine crusts rich in manganese and iron. Geol. Soc. Am. Bull. 91, 44–54.

Usui, A., Someya, M., 1997. Distribution and composition of marine hydrogenetic and hydrothermal manganese deposits in the northwest Pacific, in: Nicholson, K., Hein, J.R., Buhn, B., Dasgupta, S. (Eds.), Manganese Mineralization Geochemistry and Mineralogy of Terrestrial and Marine Deposits. Geol. Soc. Publ. 119, 177–198.

Varentsov, I.M., 1962. On the main manganese-bearing formations, in: Sedimentary Iron-Manganese Ores (Trans. GIN, Issue 70) [in Russian]. GIN, Moscow, pp. 119–161.

Vasil'ev, E.P., Reznitsky, L.Z., Vishnyakov, V.N., Nekrasova, E.A., 1981. The Slyudyanka Crystal Complex [in Russian]. Nauka, Novosibirsk.

Winter, G.A., Essene, E.J., Peacor, D.R., 1981. Carbonates and pyroxenoids from the manganese deposit near Bald Knob, North Carolina. Am. Mineral. 66, 278–289.

Zaikova, E.V., 1991. Siliceous Rocks of Ophiolitic Associations: Mugodzhar Example [in Russian] Nauka, Moscow.